DEBRE BERHAN UNIVERSITY

COLLEGE OF ENGINEERING

CHEMICAL ENGINEERING DEPARTMENT

Fabrication of Ceramic Capacitor from Metal Oxides (ZrO_2, TiO_2 & BaO) and Geominerals from the North Shewa Zone (Clay & Bentonite)

By: Lidiya Mitiku kenea

December 2022

Debre Berhan, Ethiopia

DEBRE BERHAN UNIVERSITY

COLLEGE OF POST GRADUATE

Fabrication of Ceramic Capacitor from Metal Oxides (ZrO_2, TiO_2 & BaO) and Geominerals from the North Shewa Zone (Clay & Bentonite)

A Thesis Submitted to the Department of Chemical Engineering, College of Engineering Debre Berhan University

In partial Fulfillment of the Requirements for the Degree of Master of Science in Chemical Engineering (Process Engineering)

Lidiya Mitiku kenea

Advisor: Amha Betemariam (Ph.D.)

Dec. 2022

Debre Berhan, Ethiopia

DEBRE BERHAN UNIVERSITY

COLLEGE OF ENGINEERING

We, the undersigned members of the board of the examiners of the final open defense by Lidiya Mitiku Kenea have read and evaluated her thesis entitled: "*Fabrication of Ceramic Capacitor from Metal Oxides (ZrO_2, TiO_2 & BaO) and Geominerals from the North Shewa Zone (Clay & Bentonite)*", and examined the candidate. This is therefore to certify that the thesis/dissertation has been accepted in partial fulfillment of the requirements for the degree of Master of Science in Chemical Engineering.

_____	_____	_____
Name of the Chairperson	Signature	Date
_____	_____	_____
Name of Principal Advisor	Signature	Date
_____	_____	_____
Name of Internal Examiner	Signature	Date
_____	_____	_____
Name of External Examiner	Signature	Date

DECLARATION

This thesis has been submitted in partial fulfillment of the requirements for Master of Science (MSc) at Debre Berhan University. I declare that this thesis is my genuine work, and that all sources of the materials used for this thesis have been greatly recognized. I, the undersigned, Lidiya Mitiku , declare that this study entitled "Fabrication of Ceramic Capacitor from Metal Oxides (ZrO_2, TiO_2 & BaO) and Geominerals from the North Shewa Zone (Clay & Bentonite)" is the research I undertook independently with the guidance and support of my advisor. This study has not been submitted for any degree, diploma or certificate program in this or any other institution.

Declared by

Name: Lidiya Mitiku

Signature: _____

Date: ____/___/2022

Place: Debre Berhan, Ethiopia

ACKNOWLEDGEMENTS

First of all, I would like to express my deepest gratitude to the Almighty God who gave me the strength, protection, love and opportunity throughout this thesis work. The completion of this thesis work would not be possible without the support of my family, especially my father, my mother and my beloved husband. I would like to express my respect, appreciations and love for my family for their assistance, support and encouragement.

I would like to express a bottom of heart gratitude to my advisor Dr. Amha Betemariam for his valuable advice, direction, and inspiration throughout the completion of this thesis.

I highly appreciate and give thanks to Adama science and Technology University (ASTU), especially Materials Science and Engineering department Office administrative workers, teachers, and all the laboratory staff, especially Henok and Demeke for providing me all laboratory facilities and for their guidance and spending for me their precious time. I would also like to acknowledge Addis Ababa University Amist Kilo Campus especially electrical engineering department for providing me all laboratory facilities and for their guidance.

TABLE OF CONTENTS

LIST Of TABLE viii

LIST OF FIGURE ix

ABBREVIATIONS AND ACRONYMS xi

LIST OF TABLES IN THE APPENDIX xii

LIST OF FIGURES IN THE APPENDIX xiii

Abstract xiv

CHAPTER ONE 1

1. Introduction 1

1.1. Backgrounds 1

1.2. Statement of the Problem 3

1.3. Objectives 4

1.3.1. General Objectives 4

1.3.2. Specific Objectives 4

1.4. Significance of the Study 5

1.5. Scope of the Study 6

Chapter Two 7

2. Literature Review 7

2.1. Introduction to Ceramic Capacitors 7

2.2. Titanium Dioxide 8

2.3. Ceramic Capacitors 9

2.4. Ceramic Manufacturing Process 11

2.5. Strength of Ceramics 14

2.6. Theory of Chemical Processing 15

CHAPTER THREE 17

3. Materials and Methods 17
3.1. Material and Equipment Used During Experiment 17
3.1.1. Materials 17
3.1.2. Equipment used during experiment 17
3.2. Source of Geo-materials 17
3.3. Experimental location 18
3.4. Methods 19
3.4.1. Geo Mineral Preparation 19
3.4.2. Green-Mass Formulation 19
3.5. Experimental procedure 19
3.5.1. Design of experiments (DoE) 19
3.6. Ceramic Capacitor Production process 21
3.6.1 Mixing 21
3.6.2 Green Body preparation 22
3.6.3 Drying 22
3.6.4 Firing 22
3.7. Testing of Physical Properties of Ceramics Capacitors Samples 22
3.7.1. Bulk Density 23
3.7.2. Apparent Porosity 23
3.7.3. Water absorbance 24
3.7.4. Linear shrinkage 24
3.8. Mechanical Properties Testing 24
3.8.1. Vickers Hardness Testes 24
3.9. Dielectric Strength 25
3.10. X-ray Diffraction (XRD) Analysis 26

CHAPTER FOUR 27
4. RESULTS AND DISCUSSION 27
4.1. Raw material Characterization 27
4.2. Experimental Results 28
4.3. Development of Empirical Models 28
4.4. Adequacy Check for the Developed Models 29
4.5. Effect of Process Parameters on Dielectric Strength 33
4.5.1. Perturbation Plot 33
4.5.2. One Factor Plot 34
4.5.3. Interaction Effects 35
4.5.4. 3D Surface and contour plot for dielectric strength 36
4.6. Optimization 37
4.7. Validation of the Developed Models 40
4.8. Mechanical Property of ceramic capacitors samples 41
4.8.1. Vickers hardness of ceramic capacitors samples 41
4.9. Physical Properties of Ceramic Capacitors Samples 44
4.9.1. Bulk Density of Ceramic Capacitor analysis 44
4.9.3. Linear Shrinkage of Ceramic Capacitor Analysis 47
4.10. X-ray Diffraction (XRD) Analysis 48
CHAPTER FIVE 50
5. CONCLUSION AND RECOMMENDATION 50
5.1. Conclusion 50
5.2. Recommendation 51
REFERENCES 52
APPENDIXES 55

LIST Of TABLE

Table2. 1 Properties of various modification of titanium dioxide 8
Table2. 2 Chemical composition of TiO_2 of various grades Wt. % 9
Table2. 3 Some electro-physical properties of crystalline phases of capacitor ceramics 10
Table3. 1 The compositions of the green mass body 19
Table3. 2 The factors, unite and general levels used for general factorial design 20
Table3. 3 Sequential models fitting for process variables 21
Table4. 1 The chemical composition of Clay and Bentonite clays 27
Table4. 2 The dielectric strength of all experimental runs 28
Table4. 3 ANOVA results for the response dielectric strength 30
Table4. 4 Value of PRESS, R- Squared, Adj R- Squared, Pred R- Squared, Adeq Precision 30
Table4. 5 Constraints to optimize the dielectric strength 38
Table4. 6 Other optimum conditions at different factors 39
Table4. 7 Predicted and actual values of dielectric strength and percentage error 41

LIST OF FIGURE

Figure3. 1 The experimental process flow diagram of the study..... 18
Figure4. 1 Normal plot of residuals for dielectric strength..... 31
Figure4. 2 Residuals vs. predicted graph of dielectric strength..... 31
Figure4. 3 A) Residual vs. sintering temperature and B) residual vs. pressing pressure..... 32
Figure4. 4 Box-Cox plot for power transforms Lambda=1 current=0.5 best=-2.64 32
Figure4. 5 Predicted vs. actual plot of dielectric strength..... 33
Figure4. 6 Perturbation plot for dielectric strength (A=sintering temperature, B=pressing pressure and C=soaking time)..... 34
Figure4. 7 One factor plots for dielectric strength (effect of sintering temperature on dielectric strength) 35
Figure4. 8 Interaction graph of dielectric strength (X=B: pressing pressure Y=Soaking time)... 35
Figure4. 9 Three-dimensional 3D response surface and contour plot showing the effect of sintering Temperature, Pressing Pressure and Soaking Time fixed at 2.00 Hr. A) Contour and B) 3Dsurface response respectively..... 37
Figure4. 10 Ramp plot for optimizing dielectric strength of ceramic capacitor..... 38
Figure4. 11 3D surface plot and contour plot for optimizing dielectric strength actual factor of sintering temperature 1449.84(A) contour plot and B) 3D surface plot)..... 40
Figure4. 12 Micro Vickers hardness test set-up at a temperature of 1450, pressing pressure 60 and soaking time 2 hour (Adama science and technology university in a material engineering lab, Ethiopia)..... 42
Figure4. 13 Micro Vickers hardness test set-up at a temperature of 1450, pressing pressure 40 and soaking time 2 hour (Adama science and technology university in a material engineering lab, Ethiopia)..... 42
Figure4. 14 Micro Vickers hardness test set-up at a temperature of 1450, pressing pressure 50 and soaking time 3 hour (Adama science and technology university in a material engineering lab, Ethiopia)..... 43
Figure4. 15 Micro Vickers hardness test set-up at a temperature of 1350, pressing pressure 50 and soaking time 3 hour (Adama science and technology university in a material engineering lab, Ethiopia)..... 43
Figure4. 16 Bulk Density (g/ml) of the ceramic sample as a function of pressing pressure 44

Figure4. 17 Bulk Density (g/ml) of the ceramic sample as a function of soaking time 45
Figure4. 18 Bulk Density (g/ml) of the ceramic sample as a function of sintering temperature.. 45
Figure4. 19 Water Absorbance of the ceramic capacitor sample as a function of sintering temperature 46
Figure4. 20 Apparent Porosity of the ceramic capacitor sample as a function of sintering temperature 46
Figure4. 21 Linear shrinkage of ceramic capacitor sample as function of pressing pressure 47
Figure4. 22 Linear shrinkage of ceramic capacitor sample as function of soaking time..... 47
Figure4. 23 Linear shrinkage of ceramic capacitor sample as function of sintering temperature 48
Figure4. 24 Powder X-ray diffraction pattern of ceramic capacitor at sintering temperature of 1400°c 49

ABBREVIATIONS AND ACRONYMS

ASTU……..Adama science and technology university

SEM ……scanning electron microscope

XRD……X-Ray Diffraction

ASTM..... American Standard for Testing Material

RF……Radio Frequency

HIP……..Hot Isostatic pressing

CVD ……Chemical Vapor Deposition

DoE .....Design of Experiments

RSM…….....Response surface methodology

BBD……..Box-Behnken design

ANOVA…….....Analysis of Variance

2FI .....Two Factors Interaction

HV……Vickers pyramid number

FWHM…… full width at half maximum

LIST OF TABLES IN THE APPENDIX

Table A1. 1 Effect of sintering temperature on water absorbance, bulk density and apparent porosity. 55
Table A1. 2 Effect Soaking Time on water absorbance, bulk density and apparent porosity. 55
Table A1. 3 Effect Pressing Pressure on water absorbance, bulk density and apparent porosity. 55
Table A1. 4 Water absorption of all samples. 56
Table A1. 5 Apparent porosity of all sample 57
Table A1. 6 Bulk density data of all samples. 58
Table A1. 7 Effect of pressing pressure on linear shrinkage 58
Table A1. 8 Effect of sintering temperature on linear shrinkage 58
Table A1. 9 Effect of soaking time on linear shrinkage 59
Table A1. 10 Linear shrinkage data of all samples 59
Table A1. 11 Result of all Dielectric strength [KV/mm] data 60
Table A1. 12 Vickers Hardness (MPa) and tensile strength (MPa) of all data. 61

LIST OF FIGURES IN THE APPENDIX

Figure A4 1 Three-dimensional 3D response surface and contour plot showing the effect of sintering Temperature and Pressing Pressure and Soaking Time fixed at 2.00 Hr. A)Contour and B) 3Dsurface response respectively. 69
Figure A4 2 Three-dimensional 3D response surface and contour plot showing the effect of Soaking Time and Pressing Pressure and Sintering Temperature fixed at 1400°c A) contour and B) 3Dsurface response. 70
Figure A4 3 Three-dimensional 3D response surface and contour plot showing the effect of Soaking Time and Sintering Temperature and Pressing Pressure fixed at 50KPa A) contour and B) 3Dsurface response. 71
FigureA5. 1 Vickers Hardness Tester for measuring the hardness of the sample 72
FigureA5. 2 Suspended mass measurement in the laboratory 72
FigureA5. 3 The sample boiled in the distilled water 73
FigureA5. 4 The sample in the furnace 73
FigureA5. 5 The sample after sintering and the powder weigh up in electrical balance 74
FigureA5. 6 The sample molded in the press mold and pressed specimens. 74
FigureA5. 7 Ball mill machine for milling and mixing 75
FigureA5. 8 The specimen in forced convection drying oven 75

Abstract

Ceramic capacitors are fixed-value capacitors made of ceramic material as the dielectric. Ceramic capacitors are one of the most promising electrical energy storage technologies due to their fast storage capacity, long cycle stability, high power density and environmental friendliness. In this work, the researcher investigated the production of ceramic capacitor material from metal oxides and geominerals found in the North Shewa zone of Ethiopia's Amhara region. At a proportion of Titanium dioxide 32%, Zirconium (IV) oxide 46.1%, Barium Oxide 6.9%, Bentonite 4.9% and Clay 9.8%. The chemical compositions of the Bentonite and Clay were characterized by the Classical silicate analysis method. The effect of pressing pressure, sintering temperature and soaking time was determined for each test sample and the electrical properties of the ceramic capacitor were studied in this research. The specimen was compacted at different pressing pressures from 40 MPa to 60 MPa. The green mass dried overnight in the oven at 100 ℃. The specimen was sintered at different temperatures from 1350℃ to 1450℃ for 1 hr. to 3 hrs. at a soaking firing rate of 5 ℃/minute. The produced ceramic capacitors were characterized in terms of bulk density (2.6346g/ml-3.5307g/ml), apparent porosity (1.8395%-10.1182%), water absorption (0.5439%-3.0611%), linear shrinkage (5.1098%-12.89%), Vickers hardness (KgF/mm2) (329-425.9), and dielectric strength (54.49 kv/mm-74.94kv/mm). the validation of the developed models was determined. To optimize the dielectric strength of the ceramic capacitor sample, the optimum process parameters are at a sintering temperature of 1449.85℃, pressing pressure of 57.9 MPa and soaking time of 2.87hrs. The microstructural investigation of the ceramic capacitor for this work was carried out by XRD.

Key Words: Capacitor; Sintering; Optimization and Microstructure

CHAPTER ONE

1. Introduction

1.1. Backgrounds

A Capacitor is simply a device which stores charge. Since the beginning of electrical research, non-conductive materials such as glass, porcelain, paper and mica have been used as insulators. Decades later, these materials were also suitable as dielectrics for the first capacitors. Since the early days of Marconi radio transmitters, porcelain capacitors have been used for high voltage, high frequency applications in transmitters. On the receiver side, a small mica capacitor was used in the resonant circuit. Dielectric mica capacitors were invented by William Duvilliers in 1909. Mica is a natural material and is limited in quantity. Thus, in the mid-1920s, a shortage of mica in Germany and the experience of porcelain, a special class of ceramics, resulted in the first German capacitors using ceramics as a dielectric, founding a new family of ceramic capacitors[1].

Some crystalline substances have an increased, high, and even ultra-high value of the dielectric constant, reaching several thousand. Such substances are used for the production of ceramic products for special purposes, the so-called capacitor. Such crystalline substances include titanium dioxide, a large amount of titanates ($MeTiO_3$), zirconates ($MeZrO_3$), niobates ($MeNb_2O_3$), and some other compounds[2].

The main raw material for the manufacture of ceramic materials used in the manufacture of capacitors is titanium dioxide, which has a relatively high value of dielectric constant. Ceramic materials for capacitors, the crystalline basis of which is TiO_2 and some titanates, are called ticonds. A significant disadvantage of titanium dioxide ceramics is a large negative Tkε, which, with increasing temperature, changes the capacitance of capacitors made from this ceramic. The decrease in Tkε in ceramics capacitor is achieved by introducing into the composition some compounds that independently have a positive Tkε or during firing form new crystalline phases with TiO_2, which also have a positive Tkε. Such additives that reduce the Tkε of purely rutile ceramics are ZrO_2 and BaO, which form compounds with positive Tkε. The interaction of such types

of oxides with TiO_2, as a result of which certain crystalline phases should form. The most important crystalline phase compounds synthesized for the production of ceramic capacitor include $BaTiZrO_3$, $CaTiO_3$, $ZrTiO_4$, etc.[2].

The introduction of a fairly significant amount of clay and Bentonite substances into the ceramic mass, which simultaneously acts as a binder during molding and control the dielectric constant values of the ceramic capacitor. A small amount of BaO is added in the ceramic composition mixture through $BaCO_3$, which, interacting with clay substances, forms barium aluminosilicate glass with a positive Tkε[3].

The global demand for ceramic capacitors is skyrocketing as a result of technological advancements in communication for products such as radio, television, telephone, biomedical equipment, and all electronics appliances. Thus finding various mineral deposits such as metallicores, Bentonite and clays raw materials is critical.

Capacitor manufacturing technology has not yet been introduced in Ethiopia, limiting experience in this field of research. This study attempted to prepare ceramic capacitor materials from geo-minerals found in Ethiopia's north shewa region (Clay and Bentonite), as well as metallic oxides such as Titanium dioxide, Zirconium dioxide, and Barium dioxide.

1.2. Statement of the Problem

Mineral deposit naturally available in Ethiopia includes such as Clay and Bentonite which are very useful for manufacturing of ceramic capacitor. The demand for ceramic capacitor is alarmingly increasing worldwide as a result of technological advancement in communication for such products as radio, television, telephone, biomedical equipment and for all electronics appliances. Based on Volza's Ethiopia Import data, Ethiopia imports most of its Capacitors from India, China and Italy. Ethiopia Imports of capacitor were US$60.09 Million during 2021, according to the United Nations COMTRADE (Common format for Transient Data Exchange for power systems) database on international trade. Ethiopia is the largest importer of Capacitors and accounts for 801 shipments. However Ethiopia, especially Amhara region is endowed with the most important minerals for manufacturing of ceramic capacitors but the country is importing huge amount of ceramic capacitors which requires huge amount of hard currency. Therefore, the manufacture of ceramic capacitor domestically would enable foreign currency savings and develop the country's capacity to lay ground for technological advancement. Therefore this study focuses on the manufacturing of ceramic capacitor using TiO_2, ZrO_2, $BaCO_3$ and geominerals that are available in Amhara region (Clay and Bentonite).

1.3. Objectives

1.3.1. General Objectives

The main objective of this study was to manufacture ceramic capacitor from Titanium dioxide,

Zirconium oxides, Barium carbonate and Geo-mineral deposits (Bentonite and Clay) in Ethiopia, Northern Shewa, Amhara region.

1.3.2. Specific Objectives

- To investigate the chemical composition of geominerals using the classical silicate analysis
- To study the effect of the process parameters such as sintering temperature, soaking time and pressing pressure on dielectric strength properties of ceramic capacitors.
- To optimize the process parameters for the optimum dielectric strength properties of ceramic capacitors.
- To characterize the chemical, physical, mechanical and electrical properties of the ceramic capacitor.

1.4. Significance of the Study

The study provides the production of ceramic capacitor from Titanium dioxides, Barium carbonate, Zirconium oxides and locally available raw material. The work will lighten the suitability of using Ethiopian mineral deposits as raw materials for the production of ceramic capacitors. This study will minimize the imported product of ceramic capacitor from different parts of the world. The electronics equipment in Ethiopia is increased alarmingly, therefore the need for capacitor are also increased. This study will reduce the imported ceramic capacitor grown and the demand of which can be covered at an affordable price domestically. Additionally this study will be used as a baseline for future research to produce quality ceramic capacitor from locally available raw material.

1.5. Scope of the Study

The study focused on the production of ceramic capacitor from Titanium dioxides, Barium carbonate, Zirconium oxides and locally available raw material. As concerned with geographical scope the study focused only on Amahara National regional state of North Shoa Zone. The effect of the process parameters such as sintering temperature, soaking time and pressing pressure were accounted for on the dielectric strength of ceramic capacitor. The chemical, physical, mechanical and electrical properties of the ceramic capacitor were characterized. The scope of the study is limited to the total number of 17 run of experiment.

Chapter Two

2. Literature Review

2.1. Introduction to Ceramic Capacitors

The ceramic capacitor is the foremost broadly utilized passive component in advanced electronics. In 2008, it accounted for ~90% of the capacitor showcase in portion volume and ~40% in value[4]. The multilayer ceramic capacitor (MLCC), characterized by its tall capacitance and compactness, is the overwhelming frame of ceramic capacitor. With hundreds of MLCCs utilized in ordinary electronic devices such as cell phones and computers, roughly 1.5 trillion pieces of MLCC were made in 2009, and in overabundance of 2 trillion pieces will be fabricated in 2011[5].

The innovative significance of the ceramic capacitor is not limited to MLCCs. Specialty ceramic capacitors with distinctive capabilities cover performance gaps in other capacitor technologies, e.g., high-temperature capacitors up to several hundred degrees Celsius and single-element high voltage capacitors that withstand 50 to 100 kV[4].

A wide variety of ceramic materials with a wide range of dielectric properties can be utilized to manufacture capacitors. Modern ceramic dielectrics have a dielectric constant (K) that spans a range from as low as 5 to greater than 20,000, while temperature dependence ranges from a number of ppm/°C to 1%/°C. Commercially available ceramic dielectrics are categorized into three classes:

Class I Dielectrics

Class I dielectrics are low K (dielectric constant) (5 to a few hundred) ceramics with low dissipation factor (<<0.01). Most early dielectric ceramics have a place to this class, including porcelain, steatite (talc), mica, and other silicates. Nowadays, most Class I dielectrics are based on simple oxides, e.g., TiO_2 (rutile), and perovskite titanates, e.g., $CaTiO_3$ and altered $(Ca,Sr)(Zr,Ti)O_3$. Polycrystalline rutile includes a dielectric constant of ~100 and a temperature coefficient of approximately −750 ppm/°C but can be blended with other Class I dielectrics to realize tailored dielectric performance[4].

Class II dielectrics

Class II dielectrics are high K (dielectric constant) materials (1,000 to >20,000). Barium Titanate. Barium titanate ($BaTiO_3$), discovered at the same time in several nations during WWII [4], is the first simple metal oxide compound in which ferroelectric behavior was observed. The ferroelectricity in $BaTiO_3$ gives rise to high permittivity (maximum K >10,000) that was orders of size greater than any existing dielectric at that time. The technological significance of the material was recognized immediately, and broad investigate to adjust its dielectric behavior ensued. More than 60 a long time afterward, barium titanate is still the base material of choice for ceramic dielectrics[4].

Class III dielectrics

Class III dielectrics are the basis for barrier layer capacitors. Through a reduction-reoxidation process, each grain within the dielectric comprises of a conductive core and a thin insulating shell, or barrier layer. When voltage is applied to the dielectric, the electric field concentrates in the thin barrier layer, which comes about in extremely high capacitance but low operating voltage (usually <25V)[4].

2.2. Titanium Dioxide

The main raw material for ceramic capacitor is titanium dioxide (TiO_2) which has a relatively high dielectric constant. In its pure form, TiO_2 is almost never found in nature, chiefly minerals of titanium dioxide are limonite $FeTiO_3$, $CaTiSiO_5$, and $CaTiO_3$ and etc. Titanium Dioxide exists in three modification forms Anatase, Brookite and Rutile (Table2.1).

Table2. 1 Properties of various modification of titanium dioxide

Type of Modification	Crystal System	Density , g/cm3	Melting point	Molar volume
Anatase	Tetragonal	3.9	Transformation to rutile	19.377
Brookite	Pombic	3.9-4	Transformation to rutile	20.156
Rutile	Tetragonal	4.2-4.3	1830-1850	18.693

Rutile is a stable high temperature form, into which the first two forms of TiO_2 irreversibly transform upon heating. Titanium dioxide is widely used in the metallurgy of hard alloys in the pro-

duction of electrodes, as a pigment for dyes in the varnish and paint industry, and for other purpose. The requirements for TiO_2 are very different for these consumers. For the ceramic industry, a special grade TiO_2 is produced and it is called a capacitor grade. Titanium dioxide for various purposes has different chemical purity and dispersion, which can have a certain effect on the properties of rutile ceramics. Table2.2 shows the approximate chemical compositions of some grades of titanium dioxide[4, 5].

Table2. 2 Chemical composition of TiO_2 of various grades Wt. %

Type	**TiO_2**	**Fe_2O_3**	**P_2O_3**	**SiO_2**	**Moisture**
Capacitor	99	0.1	0.05	0.28	0.5
Electrode	97.5	0.15	-	0.2	0.65

The dielectric constant of polycrystalline rutile relatively low and equals 114 Rutile has a very large negative temperature coefficient of dielectric constant TKe, equal to -750 $x10^{-6}$ deg^{-1}. The first ceramic capacitors were fabricated on the basis of TiO_2, having a very high capacitance at that time[8, 9].

2.3. Ceramic Capacitors

Ceramics materials from which capacitors with high capacitance stability are made are called thermoconds (thermo stable capacitors). Thermocondes have a lower dielectric constant than ticondes and have a small positive negative coefficient or dielectric decrease in TKε in thermal conduits is achieved by introducing into composition of the ceramic mass some compounds that independently a positive TKε or from new crystals with TiO_2 during firing ,form new crystalline phases with TiO_2, which also have a positive TC. Thus, the total TKε of several crystalline phases formed in the fired ceramic capacitor [1, 10] .

Such added substances that diminish TC of purely rutile ceramics are earth metal oxides , Which form compounds with positive TKε .With the introduction of the corresponds compounds , most often in the form of oxides , an interaction with TiO_2 occurs , as a result of which certain crystalline phases should be formed . The most important compounds synthesized for the production of

titanium capacitor ceramics and some of their electrophysical properties are given in Table2.3 [1].

Table2. 3 Some electro-physical properties of crystalline phases of capacitor ceramics

Formula	ε **(Dielectric constant)**	TKε.10^6 **(Dielectric Permeability)**	**tg**δx10^4 **(Dielectric lose)**
$SrTiO_3$	250	-2500	2
$CaTiO_3$	150	-1500	3
TiO_2	90	-800	10
$BaZrO_3$	38	-350	-
$ZrTiO_4$	40	-100	5

The best compositions can contain as it wereTiO_2 and, as a plasticizer, refractory plastic clay in variable amounts, in this case, it is possible to obtain a number of materials with a decreasing value of as the clay mass increases, the dielectric constant whose bridge is 7. Among other compounds, $ZrTiO_4$ is of great importance in the system ZrO_2-TiO_2; there is only one double compound, namely ortho zirconium titanate. For the fabrication of condenser ceramics, not only the orthotite zirconium itself is important, but also the compositions laying the region of solid solutions of the $ZrTiO_4$ & TiO_2 system [11].

A typical mass for the manufacture of thermo stable capacitors (thermoconductors) is the mass of ceramic capacitor. The crystalline phase of the mass is $ZrTiO_4$, which is synthesized from TiO_2 and ZrO_2 included in the mass, during the firing process[6, 10].

The dielectric constant of $ZrTiO_4$ is 40. Due to the introduction into the mass of a rather significant amount of clay substances, which simultaneously act as a binder during molding, the dielectric constant of the ceramic capacitor mass decreases to 18-24, A small amount of BaO is added to the composition of the ceramic capacitor mass through $BaCO_3$, which, interacting with clay substances, forms barium-aluminosilicate glass with a positive TKε. In the production of capacitor ceramics, in most cases, crystalline phases are preliminary synthesized in powders or briquettes (cakes). The need for such a synthesis is due to large shrinkage of the masses, abundant

gas release from decomposing salts (for example, carbonates), which entails unacceptable deformation included in the mass is carried out. Only in some cases it is possible to synthesize these masses directly in the product with its single crimping[12] 10] .

Until recently , under industrial conditions , the synthesis of crystalline phases or solid solutions included in the capacitor ceramics of compounds was carried out only by high temperature calcination of a mixture of the corresponding oxides or sometimes salts, for example carbonates. During firing, solid phase reactions predominate. However, in some cases, the liquid phase formed during firing also plays a role [1].

Long term practice has shown that the phase composition synthesized from ceramic oxides is not stable , since it depends on many difficult and precisely controlled technological factors , for example, fluctuations in the amount of impurities in the raw material, preliminary heat treatment of raw materials, grinding, conditions of product design, temperature fluctuation, etc. firing environments and other causes [13].

2.4. Ceramic Manufacturing Process

The ceramic manufacturing process generally follows this sequence:

Milling → Batching → Mixing → forming → Drying → firing → Assembly [14].

Milling is the mechanical process by which materials are reduced from a large size to a smaller size. Milling may involve breaking up of material (in which case individual particles retain their shape) or pulverization (which includes smashing the particles themselves to a diminished estimate).

Batching is the process of weighing the oxides agreeing to formulas, and planning them for blending and drying.

Mixing Blending happens after clustering and is performed with different machines, such as dry mixing ribbon mixers (a type of cement mixer), Mueller mixers, and pug mills. Wet mixing generally involves the same equipment.

Forming Shaping is making the blended fabric into shapes, ranging from toilet bowls to spark plug insulators. Forming can include:

(1) Extrusion, such as extruding "slugs" to make bricks,

(2) Pressing to make shaped parts,

(3) Slip casting, as in making toilet bowls, wash basins and ornamentals like ceramic statues. Forming produces a "green" part, ready for drying. Green parts are soft, pliable, and over time will lose shape. Handling the green product will change its shape. For example, a green brick can be "squeezed", and after squeezing it will stay that way.

Drying is evacuating the water or binder from the shaped material. Spray drying is broadly utilized to get ready powder for squeezing operations. Other dryers are tunnel dryers and occasional dryers. Controlled heat is connected in this two-stage handle. To begin with, heat evacuates water. This step needs cautious control, as quick warming cause's splits and surface defects. The dried portion is littler than the green part, and is delicate, requiring careful taking care of, since a little impact will cause disintegrating and breaking.

Firing is a process of evacuating the water or other binder from the formed ceramic material where the dried parts pass through a controlled heating process, and the oxides are chemically changed to cause sintering and bonding. The fired portion will be diminished their size.

Forming methods

Ceramic shaping methods incorporate throwing, slip casting, tape molding, injection molding, dry pressing, isostatic pressing, hot isostatic pressing (HIP) and others. Methods for forming ceramic powders into complex shapes are desirable in many areas of technology. Such methods are required for producing an advanced, high-temperature structural parts such as heat engine components and turbines. Materials other than ceramics which are used in these processes may include: wood, metal, water, plaster and epoxy—most of which will be eliminated upon firing. These forming techniques are well known for providing tools and other components with dimensional stability, surface quality, high (near theoretical) density and microstructural uniformity. The expanding utilize and differing qualities of strength shapes of ceramics includes to the differing qualities of handle innovations to be utilized [11].

Thus, reinforcing fibers and filaments are mainly made by polymer, sol-gel, or CVD processes, but melt processing also has applicability. The most widely used specialty form is layered struc-

tures, with tape casting for electronic substrates and packages being pre-eminent. Photolithography is of increasing interest for precise patterning of conductors and other components for such packaging. Tape casting or forming processes are also of increasing interest for other applications, ranging from open structures such as fuel cells to ceramic composites [15].

The other major layer structure is coating, where melt spraying is very important, but chemical and physical vapor deposition and chemical (e.g., sol-gel and polymer pyrolysis) methods are all seeing increased use. Besides open structures from formed tape, extruded structures, such as honeycomb catalyst supports, and highly porous structures, including various foams, for example, reticulated foam, are of increasing use [15].

Densification of consolidated powder bodies continues to be achieved predominantly by (pressure less) sintering. However, the use of pressure sintering by hot pressing is increasing, especially for non-oxides and parts of simple shapes where higher quality (mainly microstructural homogeneity) is needed and larger size or multiple parts per pressing can be an advantage [15].

The sintering process

The standards of sintering-based strategies are basic. The firing is done at a temperature underneath the melting point of the ceramic. Once a roughly-held-together object called a "green body" is made, it is heated in a furnace, where atomic and atomic diffusion processes deliver rise to significant changes within the essential microstructural features. This includes the gradual elimination of porosity, which is typically accompanied by a net shrinkage and overall densification of the component. Thus, the pores in the object may close up, resulting in a denser product of significantly greater strength and fracture toughness [16].

Another major change in the body during the firing or sintering process will be the establishment of the polycrystalline nature of the solid. This change will make known to some form of grain size distribution, which will have a significant impact on the ultimate physical properties of the material. The grain sizes will either be associated with the initial particle size, or possibly the sizes of aggregates or particle clusters which arise during the initial stages of processing [15].

The ultimate microstructure (and thus the physical properties) of the final product will be limited by and subject to the form of the structural template or precursor which is created in the initial

stages of chemical synthesis and physical forming. Hence the importance of chemical powder and polymer processing as it pertains to the synthesis of industrial ceramics, glasses and glass-ceramics [17].

There are numerous possible refinements of the sintering process. Some of the most common involve pressing the green body to give the densification a head start and reduce the sintering time needed. Sometimes organic binders such as polyvinyl alcohol are added to hold the green body together; these burn out during the firing (at 200–350 °C). Sometimes organic lubricants are added during pressing to increase densification. It is common to combine these, and add binders and lubricants to a powder, then press. The formulation of these organic chemical additives is an art in itself. This is particularly important in the manufacture of high performance ceramics such as those used by the billions for electronics, in capacitors, inductors, sensors, etc.. Slurry can be used in place of a powder, and then cast into a desired shape, dried and then sintered. Indeed, traditional pottery is done with this type of method, using a plastic mixture worked with the hands. If a mixture of different materials is used together in a ceramic, the sintering temperature is sometimes above the melting point of one minor component – a liquid phase sintering. These results in shorter sintering times compared to solid state sintering [18].

2.5. Strength of Ceramics

A material's strength is dependent on its microstructure. The engineering processes to which a material is subjected can alter this microstructure. The varieties of strengthening mechanisms that alter the strength of a material include the mechanism of grain boundary strengthening. Thus, although yield strength is maximized with decreasing grain size, ultimately, very small grain sizes make the material brittle. Considered in tandem with the fact that the yield strength is the parameter that predicts plastic deformation in the material, one can make informed decisions on how to increase the strength of a material depending on its microstructural properties and the desired end effect [18].

The relation between yield stress and grain size is described mathematically by the Hall-Petch equation which is

$$\sigma_y = \sigma_0 + \frac{k_y}{\sqrt{d}} \qquad 2.1$$

Where k_y is the strengthening coefficient (a constant unique to each material), $\boldsymbol{\sigma_0}$ is a materials constant for the starting stress for dislocation movement (or the resistance of the lattice to dislocation motion), d is the grain diameter, and $\boldsymbol{\sigma_y}$ is the yield stress [16].

Theoretically, a material could be made infinitely strong if the grains are made infinitely small. This is, unfortunately, impossible because the lower limit of grain size is a single unit cell of the material. Even then, if the grains of a material are the size of a single unit cell, then the material is in fact amorphous, not crystalline, since there is no long range order, and dislocations cannot be defined in an amorphous material. It has been observed experimentally that the microstructure with the highest yield strength is a grain size of about 10 nanometers, because grains smaller than this undergo another yielding mechanism, grain boundary sliding. Producing engineering materials with this ideal grain size is difficult because of the limitations of initial particle sizes inherent to nanomaterials and nanotechnology [16].

2.6. Theory of Chemical Processing

Microstructural Uniformity

In the processing of fine ceramics, the irregular particle sizes and shapes in a typical powder often lead to non-uniform packing morphologies that result in packing density variations in the powder compact. Uncontrolled agglomeration of powders due to attractive van der Waals forces can also give rise to in microstructural in homogeneities [17].

Differential stresses that develop as a result of non-uniform drying shrinkage are directly related to the rate at which the solvent can be removed, and thus highly dependent upon the distribution of porosity. Such stresses have been associated with a plastic-to-brittle transition in consolidated bodies, and can yield to crack propagation in the unfired body if not relieved [17].

In addition, any fluctuations in packing density in the compact as it is prepared for the kiln are often amplified during the sintering process, yielding inhomogeneous densification. Some pores and other structural defects associated with density variations have been shown to play a detri-

mental role in the sintering process by growing and thus limiting end-point densities. Differential stresses arising from inhomogeneous densification have also been shown to result in the propagation of internal cracks, thus becoming the strength-controlling flaws [18] .

It would therefore appear desirable to process a material in such a way that it is physically uniform with regard to the distribution of components and porosity, rather than using particle size distributions which will maximize the green density. The containment of a uniformly dispersed assembly of strongly interacting particles in suspension requires total control over particle-particle interactions. Monodisperse colloids provide this potential[19].

Monodisperse powders of colloidal silica, for example, may therefore be stabilized sufficiently to ensure a high degree of order in the colloidal crystal or polycrystalline colloidal solid which results from aggregation. The degree of order appears to be limited by the time and space allowed for longer-range correlations to be established[20].

Such defective polycrystalline colloidal structures would appear to be the basic elements of submicrometer colloidal materials science, and, therefore, provide the first step in developing a more rigorous understanding of the mechanisms involved in microstructural evolution in inorganic systems such as polycrystalline ceramics [20].

CHAPTER THREE

3. Materials and Methods

The methodology for this research is generally experimental and it has five related stages.

I. Collection and purification of geominerals that are available in Amhara region- Clay and Bentonite.
II. Study the chemical composition of Bentonite and Clay.
III. Mass preparation & production of ceramic capacitor.
IV. Study the effect of the process parameters reaction temperature, soaking time & pressing pressure on the ceramic capacitor properties.
V. Characterize the chemical, physical, mechanical and electrical properties of the ceramic capacitor.

3.1. Material and Equipment Used During Experiment

3.1.1. Materials

The major geominerals (Bentonite and Clay) were used during the preparation of ceramic capacitor. The other three chemicals were collected from the market. Titanium dioxide, (TiO_2), Zirconium oxide, (ZrO_2), Barium carbonate, ($BaCO_3$) all this chemical were laboratory grade and the chemical are bought from chemical supplier in Addis Ababa, Ethiopia.

3.1.2. Equipment used during experiment

The equipment used for this work includes analytical balance, electrical balance, glass ware, milling machine (ball mill), sieving machine, washing machine, mixing machine, molding machine or hydraulic pressing machine, electrical oven, furnace, goggle for eyes protection, protective glove for protecting hand, ceramic properties testing machines, Electrical properties testing machines, vernier caliper, X-ray diffraction (XRD-7000S), Vickers hardness machine, wet ball mill and aluminum foil.

3.2. Source of Geo-materials

The major geominerals (Bentonite and Clay) used during the preparation of ceramic capacitor were collected from Amhara region, North Shewa zone. The Clay sample were collected from

Ankober woreda specially in Mehal Wonz and Bentonite clay collected from Merabete Woreda specially in Jemma River. The other three chemicals were collected from the market. Titanium dioxide, (TiO_2), Zirconium oxide, (ZrO_2), Barium carbonate, ($BaCO_3$) all these chemicals were laboratory grade and the chemicals are bought from chemical supplier in Addis Ababa, Ethiopia.

3.3. Experimental location

Sample preparation drying, size reduction, and particle size analysis were conducted in Debre Berhan University. And the dried, crushed and sieved out sample were produced in the experiment and product characterization is conducted in the laboratory of the Materials Science and Engineering department, Adama Science and Technology University and Addis Ababa Institution of Technology University (AAIT) physics department.

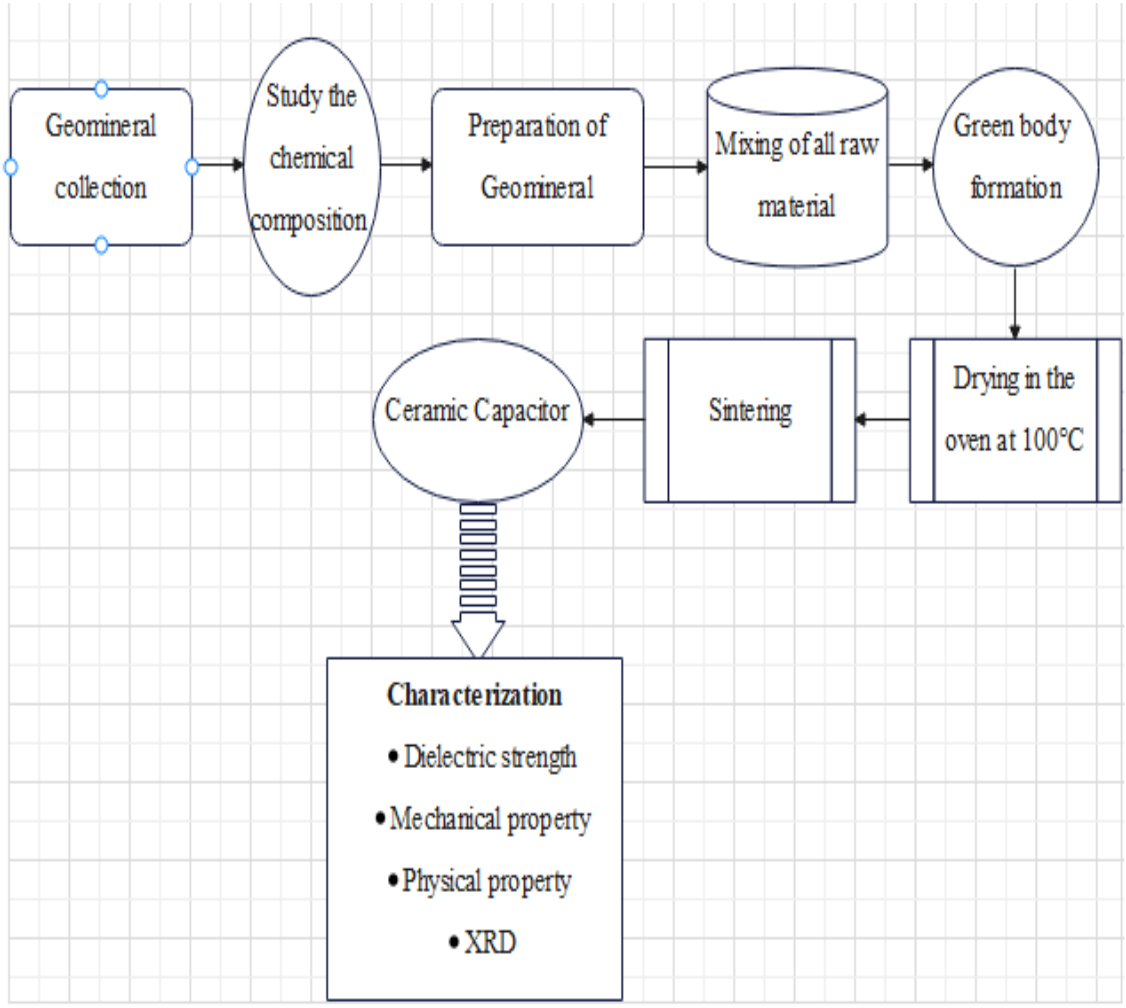

Figure3. 1 The experimental process flow diagram of the study

3.4. Methods

3.4.1. Geo Mineral Preparation

The collected raw material Bentonite and clay have many impurities. The impurities of the raw material were removed by ashing, dewatering, chemical treatment and magnetic separation operations. The purified Bentonite and clay were crushed and milled by crusher and ball mill respectively. The particle size distributions were performed by sieve analysis equipment. The particle size distributions proportions were done by granulometric calculation method to obtain required packing density.

3.4.2. Green-Mass Formulation

The purpose of calculating the composition of the raw material in the production of the material is important for the determination of the quantitative proportions of the raw component that was giving the product of the desired properties and structural compositions. The mass composition is specified in Table.3.1.

Table3. 1 The compositions of the green mass body

Materials	(Wt. %)
TiO_2	32.3
ZrO_2	46.1
$BaCO_3$	6.9
Bentonite	4.9
Clay	9.8

3.5. Experimental procedure

3.5.1. Design of experiments (DoE)

Design of experiments (DOE) was used for planning, conducting, analyzing, and interpreting controlled tests to evaluate the factors that control the value of ceramic capacitor. DOE is a powerful tool. By using DOE important interactions were identified. The main factors affecting the ceramic capacitors during the production presses is sintering temperature, pressing pressure and soaking time. All these factors are affecting the production process of ceramic capacitors. The three main factors that were selected is sintering temperature [℃], pressing pressure [MPa] and

soaking time [Hour]. The higher and the lower order were selected based on the report[21,22]. The factors selected and lower and higher order is presented in table 3.2 and in table 3. 3 factors and levels of variables used for general factorial design.

Table3. 2 The factors, unite and general levels used for general factorial design

Factor	Unit	Level		
Sintering Temperature	[℃]	1350	1400	1450
Pressing pressure	[Mpa]	80	90	100
Soaking Time	[Hr.]	1	2	3

Design Expert® software (Trial Version 6.0.8) was used to analyze and collect data from the experimental runs. Design Expert® software (Trial Version 6.0.8) is a professional statistical tool used to create the experimental design, study the effects of three factors with the least possible number of trials and optimize the designed process through simultaneous selection of the desired level of each independent variable. Box–Behnken designs that are experimental designs for response surface methodology was selected. Box-Behnken designs are used to generate higher order response surfaces using fewer required runs than a normal factorial technique. With a total number of 17 runs of experimental conditions and the response is Dielectric strength (Kv/mm). In these work the dielectric strength design is summarized, evaluated, analyzed, statistically significant of the model were determined at 5% probability level ($p < 0.05$) of analysis of variance (ANOVA) were determined. The different statistical tests were performed in the present study these are: lack of fit tests, the sequential model (sum of squares), and model summary to check the model.

Table3. 3 Sequential models fitting for process variables

Run order	Sintering Temperature [℃]	Pressing pressure [Mpa]	Soaking Time [Hr.]
1	1400	40	1
2	1450	40	2
3	1450	60	2
4	1400	50	2
5	1350	40	2
6	1350	50	1
7	1400	40	3
8	1400	50	2
9	1400	50	2
10	1400	50	2
11	1400	60	3
12	1350	60	2
13	1350	50	3
14	1450	50	1
15	1450	50	3
16	1400	60	1
17	1400	50	2

3.6. Ceramic Capacitor Production process

3.6.1 Mixing

The raw materials were weighed by using electronic balance according to the desired composition in the table 3. 1 Then the mass were positioned into a wet ball mill machine and mill by using zirconia balls (wet method) for 2 hours. Small amount of distilled water is added for homogenized mixing. The raw material should accurately mixed with finely ground granules, the ball mill were used for the mixing of the formulated samples ensuring appropriate mixing and ho-

mogenous compositions and assisted the samples to gain excellent particle interlock bonding during pressing.

3.6.2 Green Body preparation

The compacting and shaping of the mixture were done in a dry mold pressing machine Mounting Press (hand press type). Ethanol was used as a lubricating agent between the material and the mold. Poking was performed to ensure uniform pressing. Pressure was applied to the stacked mixture. Starting pressing were done with a pressure of 10 kg/cm^2 for 12 minutes to remove the entrapped air in the sample. Three groups of body were prepared and the first group was pressed maintaining a specific pressure of 40 MPa and approximates 12 Minutes of loading. The second and the third groups were molded & maintaining a specific pressure of 50 MPa and 60 MPa and approximate 12 minutes of loading respectively. The specimen size of 20 cm diameter and about 6 cm thickness were prepared by using a hydraulic press.

3.6.3 Drying

The green body or specimens were put directly into Forced Convection Drying oven used for drying wet samples for overnight at constant temperature 100℃, during drying the sample losses a required amount of moisture and the weight of the sample was changed because the moisture was removed. The water must be removed prior to sintering at high temperature. The water must be detached at a sufficiently slow rate to prevent forming of cracks and other defects.

3.6.4 Firing

The chips were fired at a temperature in the range of 1350 to 1450 degrees Celsius in the high temperature furnace. The first group samples were sintered at 1350 ℃ for a soaking period of 1hr, 2hr, and 3hrs. The second group of the samples was sintered at 1400 ℃ for a soaking period of 1hr, 2hr and 3hrs. And the last group of the sample was sintered at a temperature of 1450 ℃ for a soaking period of 1hr, 2hr and 3hrs. After sintering, the samples were characterized in terms of bulk density, water absorption, Vickers hardness, linear shrinkage, apparent porosity and dielectric strength constants.

3.7. Testing of Physical Properties of Ceramics Capacitors Samples

The physical properties of ceramic capacitor that were performed in these work is Water absorption, apparent porosity, Linear shrinkage and bulk density. And the factors that affect the physi-

cal properties (Water absorption, apparent porosity, Linear shrinkage and bulk density) were studied.

3.7.1. Bulk Density

The bulk density of a body was represented by the weight per unit volume (g/ ml) including pore space. The dry weights (Wd) of sintered ceramic capacitor samples were taken. The method used for determining the bulk density of the refractory sample was boiling method. The ceramic capacitor samples were transferred to a beaker and boiled with distilled water for 6 hours to assist in releasing trapped air. It was then allowed to soak and the saturated weight free of excess water (Ws) was taken. The specimen was then suspended in water using a beaker and the suspended weight (Wsp) was taken. The bulk density was then calculated using the relationship indicated below[23].

$$\text{Bulk density (g/ml)} = \frac{Wd}{Ws-Wsp}\ x \text{ density of water} \qquad (3.1)$$

Where, Wd = Dry weight

Ws = Saturated weight

Wsp = suspended weight

ρ_w = Density of water.

3.7.2. Apparent Porosity

Porosity is the percentage relationship between the volume of the pore space and the total volume of the sample. Apparent Porosity of the sample was using boiling method. The dry weights (Wd) of the sintered ceramic capacitor samples were taken. The dried specimen was suspended freely in distilled water and boiled for 6 hours, cooled to room temperature and its weight (Wsp) noted. The ceramic capacitor samples were transferred to a beaker and boiled with distilled water for 6 hours to assist in releasing trapped air. It was then allowed to soak and the saturated/ weight soaked weight free of excess water (Ws) was taken[23].

$$\text{Apparent Porosity (\%)} = \frac{Ws-Wd}{Ws-Wsp}\ x\ 100\ \% \qquad (3.2)$$

Where, Wd = Dry weight

Ws = Saturated weight, Wsp = suspended weight;

3.7.3. Water absorbance

The dry weights (Wd) of sintered ceramic capacitor sample were taken. The method used was determining the Water absorbance of the refractory sample was boiling method. The ceramic capacitor samples were transferred to a beaker and boiled with distilled water for 6 hours to assist in releasing trapped air. It was then allowed to soak and the saturated weight free of excess water (Ws) was taken[23].

Water absorbance (%) $=\frac{Ws-Wd}{Wd}\ x$ 100 % (3.3)

Where: Ws = soaked weight

Wd = dry weight

3.7.4. Linear shrinkage

The linear shrinkage is defined as ΔL/Lo, where Lo is the original length, L is the length at a given temperature, and Δ L=L – Lo. The dimension of the green body before firing dry length (Ld) was noted. The samples were then fired to 1350 to 1450℃ for a soaking period of, 1 hr., 2 hrs. and 3 hrs. The samples were cooled to room temperature and the fired length (Lf) was recorded. Then the linear shrinkage was calculated from the equation below[23].

Linear shrinkage = $\frac{\mathbf{Ld}}{\mathbf{Lf}}\ \boldsymbol{Ld\ x}$100 % (3.4)

Where: Ld= dry length

Lf= fired length

3.8. Mechanical Properties Testing

3.8.1. Vickers Hardness Testes

Hardness is a measure of the resistance of a material to plastic deformation induced by applied forces. Vickers hardness, a measure of the hardness of a material, calculated from the size of an impression produced under load by a pyramid-shaped diamond indenter. The Vickers hardness test were uses a square- based pyramid diamond indenter with an angle of 136° between the opposite faces at the vertex, which is pressed into the surface of the test piece using a pressed into

the surface of the test piece using a prescribed force, F. The Vickers Hardness test (ISO 6507) is used to characterize hardness of various solid materials (metals, ceramics, etc.). A diamond pyramid is pressed against the ceramic capacitor pieces with a certain normal load and the hardness is calculated based on the imprint left on the surface. A square-based pyramid indenter whose opposite sides meet at the apex at an angle of 136° is employed in Vickers hardness test.

$$HV=0.102\times 2F\left(\sin\frac{136^\circ}{2}\right)/d\text{^}2 \quad (3.5)$$

3.9. Dielectric Strength

Dielectric strength is defined as the electrical strength of an insulting material. In a sufficiently strong electric field the insulating properties of an insulator breaks down allowing flow of charge. Dielectric strength is measured as the maximum voltage required producing a dielectric breakdown through a material. It is expressed as Volts per unit thickness. For a plastic material and ceramic material the dielectric strength varies from 1 to 1000 MV/m. Dielectric strength of insulator bodies was calculated by measuring their break down voltage using high voltage testing machine (model TERCO HV 1103) at Electrical Engineering laboratory, Addis Ababa University. The positive and negative terminals of the instrument were connected at either end of the ceramic capacitor body in the oil, then the voltage was gradually increased from control disk until the voltage increment breakdown and began to drop display on control disk which indicate the break down voltage of the sample then the dielectric strength of the insulator is calculated by using Eq. (1).

$$\text{Dielectric strength} = \frac{Break\ down\ voltage\ (Kv)}{The\ thickness\ of\ the\ sample\ (mm)} \quad (3.6)$$

Where: Kv = kilovolt

mm = millimeter

3.10. X-ray Diffraction (XRD) Analysis

X-ray Diffraction (XRD) Analysis of ceramic capacitor bodies was analyzed at material Engineering department laboratory, Adama Science and Technology University (ASTU). Ceramic capacitor has been analyzed by using X-ray diffraction (X-Ray Diffractometer; XRD7000S) using Cu-Kα radiation with a voltage of 40 kV and current intensity of 30 mA at a scanning speed of 4.000deg/min, X-ray Diffraction (XRD) Analysis were used to check the nature of the materials using XRD patterns. From XRD results the crystalline (grain) size of the particles can be calculated by using the equation given below.

$$\boldsymbol{D = \frac{K\lambda}{\beta \cos\theta}} \qquad (3.7)$$

Where: D = Crystallites size (nm) =

$\boldsymbol{\beta}$ =FWHM (full width at half maximum),

θ = peak position (radians)

K = 0.9 (Scherrer constant) = 0.15406nm (wave length of the x-ray sources)

CHAPTER FOUR

4. RESULTS AND DISCUSSION

4.1. Raw material Characterization

Clay sample were collected from Ankober Woreda (Mehal Wonz) and Bentonite collected from Merabete Woreda Jemma River the Classical silicate analysis method results of Clay sample and Bentonite is given in the Table 4.1. The result showed that the oxides content of the Clay and Bentonite. The result showed that both the Clay and Bentonite mineral contain a considerably average amount of Sio_2, Al_2O_3 and Fe_2O_3.

Table4. 1 The chemical composition of Clay and Bentonite clays

minerals	Sio_2	Al_2O_3	Fe_2O_3	CaO	MgO	Na_2O	K_2O	MnO	P_2O_5	TiO_2	H_2O	LOI
Clay	54.94	19.57	3.94	0.72	0.34	<0.01	1.02	00.06	0.22	0.22	8.25	10.91
Bentonite	48.62	28.22	5.18	<0.01	0.22	<0.01	0.50	<0.01	0.06	0.27	5.03	11.01

The geochemical composition of the Clay and Bentonite samples is illustrated in Table 4.1. The results show that the most abundant oxides are silica (SiO_2) followed by alumina (Al_2O_3), iron (Fe_2O_3) and potassium (K_2O).The result showed that more siliceous (SiO_2, 48.62% - 54.94%) with significant amount of aluminum (Al_2O_3, 19.57% - 28.22%) followed by iron oxides (Fe_2O_3, 3.94% - 5.18%). Other oxides (K_2O, MgO, TiO_2, Na_2O, MnO, CaO and P_2O_5) are in somewhat lower proportion. High level of silica content explains the sandy nature of clays, these values are much closer to the values in other literatures[24]. The result showed that amount of silica (SiO_2) is considerably high and this can improve the sintering and dielectric properties of ceramics capacitor. Significant densities were increased as the SiO_2 content increased. The Raw materials were selected based on the chemical composition of the Clay and Bentonite. The chemical composition of Bentonite collected from Merabete Woreda Jemma River is good for the production of ceramic capacitors. The chemical composition of Bentonite collected from Ounda Hadar, Afar region have low SiO_2 around (52.78%)content and high contents of Fe_2O_3 (around 9.30%) if the Fe_2O_3 content increased the quality of ceramic capacitor decreases.

4.2. Experimental Results

The dielectric strength of the ceramic capacitor pieces under distinctive condition was calculated based on breakdown voltage. The experimental values of dielectric quality were displayed in table 4.2. The dielectric strength of the ceramic capacitors was related with past investigate of the dielectric capacitors of the ceramic capacitors drop within the range of 60-89Kv/mm[22,23]. The breakdown voltage and other information are displayed in appendix 1. To analyzed dielectric strength numerically and graphically the calculated value of dielectric strength were input into the design expert software version 6.0.8.

Table4. 2 The dielectric strength of all experimental runs

Run order	Sintering Temperature [°C]	Pressing pressure [Mpa]	Soaking Time [Hr.]	fired length (After sintering) [mm]	Break down voltage (Kv)	Dielectric strength [KV/mm]
1	1450	50	3.00	4.35	306	70.34
2	1450	40	2.00	4.46	318	71.30
3	1400	50	2.00	4.48	281	62.72
4	1400	40	1.00	4.49	278	61.92
5	1400	50	2.00	4.48	283	63.17
6	1400	60	3.00	4.47	294	65.77
7	1350	50	1.00	4.66	261	56.01
8	1350	50	3.00	4.63	263	56.80
9	1350	40	2.00	4.68	255	54.49
10	1400	50	2.00	4.42	269	60.86
11	1400	60	1.00	4.45	263	59.10
12	1400	40	3.00	4.51	266	58.98
13	1350	60	2.00	4.65	298	64.09
14	1400	50	2.00	4.47	266	59.51
15	1450	50	1.00	4.45	302	67.87
16	1450	60	2.00	4.35	326	74.94
17	1400	50	2.00	4.50	268	59.56

4.3. Development of Empirical Models

Design of experiments (DOE) can be defined as the systematic planning of information gathered with the use of experimental methods to identify the optimum factors and levels for this work. In this study Box- Behnken design (BBD) were used to designing experiments and optimizing the effect of process variable. BBD is one of the components of response surface methodology (RSM). In the present study BBD method were used to investigate the effect of sintering tem-

perature, pressing pressure and soaking time on the dielectric strength of the ceramic capacitor material. The fitting order for this study is 2FI and particular model selected polynomial. By using the BBD method the dielectric strength of the ceramic material is evaluated. First the selected range for transformation response was the minimum (54.49) and the maximum response was (74.94) and the ratio between maximum and minimum value is 1.3753. A ratio greater than 10 generally indicates a transformation is required, but for this study the ratio is less than 3 and the transformation had little effect. However for little effect square roots were selected. The model is evaluated to summarize whether it was fit or not. Sequential model sum of squares, lack of fit testes and model summary statistics were given in appendix2. From appendix 2, it was found that order 2FI and model polynomial that are appropriate for the Adjusted R-squared and Predicted R-squared are within approximately 0.20 of each other to be in "sound agreement." Therefore, there was no problem with either the model or the data. And the adequate precision is over 4, model provides good predictions. R-squared of 95% observed in the tangent variable is explained by the regression model, R- squared very high and fall under the accepted range. The particular model fits to each point in the design.

Model summery statistics presented lower standard deviation and lower PRESS value. The ANOVA for response surface reduced the quadratic model best fit model for this study. The ANOVA table indicated that the F- value implies the model is significant; Prob > F indicate model terms are significant because the value of Prob > F is less than 0.0500, in this case A, B, $A^{2,}$ BC were significant model terms. The lack of fit is not significant relative to the pure error. Non-significant lack of fit is good. The detail analysis of variance or ANOVA are presented in appendix 3.

4.4. Adequacy Check for the Developed Models

The adequacy of the model was checked by analysis of variance (ANOVA) statistical tests were presented. The model is significant, lack of fit insignificant. There is a reasonable agreement between Predicted R-squared and Adjusted R-squared. Adjusted and predicted R-squared values are within 0.2 of each other, Pred R-squared 0.8889 and Adj R-squared 0.9225; the difference is 0.0336 this is less than 0.2. The model provides good predictions for the average outcomes and the residuals are well behaved because Adeq Precision18.335 is greater than 4. The R-squared (R^2) indicate strength of relationship between the model and the dependent variable, R-Squared

value 0.9467 indicate the model greatly fit the data. R^2 value > 0.75 indicates the suitability of the model. For a good statistical model, the R^2 value should be close to one. R-Squared value 0.9467 shows that only 5.3% of the total variation could not be explained by the model. The Model F-value of 39.08 implies the model is significant. There is only a 0.01% chance that a "Model F-Value" and this large could occur due to noise. The values of Prob > F < 0.0001 is less than 0.0500 indicate model terms are significant. In this case A, B, A^2, BC is significant model terms. The Lack of Fit F-value is 0.76 this result implies the lack of fit is not significant. The Prob>F value is 0.6503 or 65.03% implies that Non- significant lack of fit is good. The detail analysis of variance or ANOVA are presented in appendix 3.

Table4. 3 ANOVA results for the response dielectric strength

Source	Sum of Square	DF	Mean Square	F Value	Prob>F	
Model	1.99	5	0.40	39.08	< 0.0001	Significant
A	1.74	1	1.74	170.56	< 0.0001	
B	0.056	1	0.056	5.50	0.0388	
C	0.023	1	0.023	2.30	0.1579	
A^2	0.080	1	0.080	7.83	0.0173	
BC	0.094	1	0.094	9.19	0.0114	
Residual	0.11	11	0.010			
Lack of Fit	0.064	7	9.138E-003	0.76	0.6503	not significant
Pure Error	0.048	4	0.012			
Cor Total	2.11	16				

Table4. 4 Value of PRESS, R- Squared, Adj R- Squared, Pred R- Squared, Adeq Precision

Std. Dev.	**0.10**	**R- Squared**	**0.9467**
Mean	7.89	Adj R- Squared	0.9225
C.V.	1.28	Pred R- Squared	0.8889
PRESS	0.23	Adeq Precision	18.335

Design expert in addition to ANOVA evaluate model fit and transformation choice with

graph, inspect various diagnostic plots to statistically validate the model. The normal plot of the residuals shown in Figure 4.1 It can be seen that residuals follow a normal distribution, thus follow the straight line, this implies that the models suggested are suitable. The normal plot of the residuals shows good correlation between experimental and predicted values. Figure4. 2 Residuals vs. Predicted this is a plot of the residuals versus predicted response values. Residuals vs. Predicted test the assumption of constant variance, the plot is randomly scattered (constant range of residuals across the graph). This implies that the model suggested is suitable. Figure4. 3 Residuals vs. Run showed a random scatter. Figure4. 4 Box-Cox Plot. This plot provides a guideline for selecting the correct power of low transformation. A recommended transformation is none because $\lambda = 1$ no transformation.

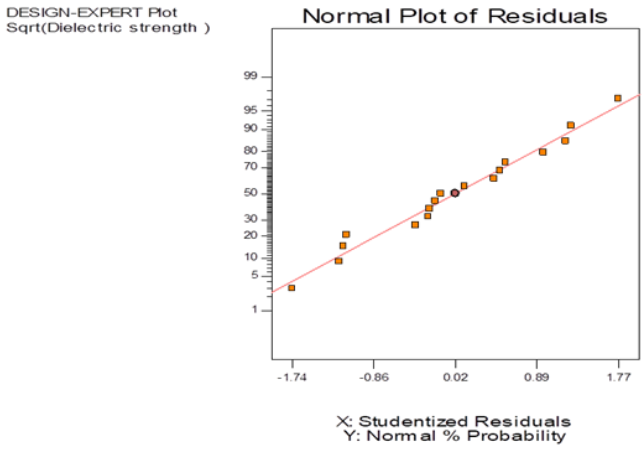

Figure4. 1 Normal plot of residuals for dielectric strength

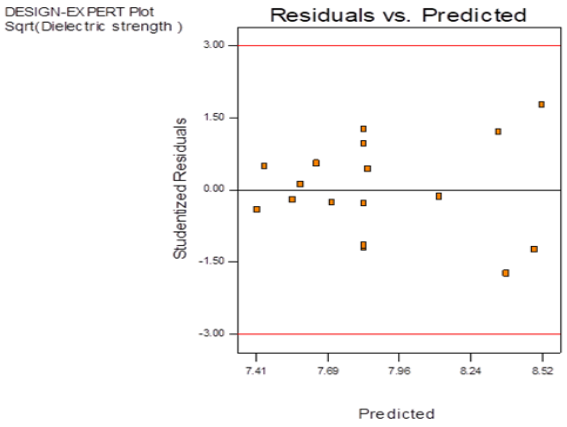

Figure4. 2 Residuals vs. predicted graph of dielectric strength

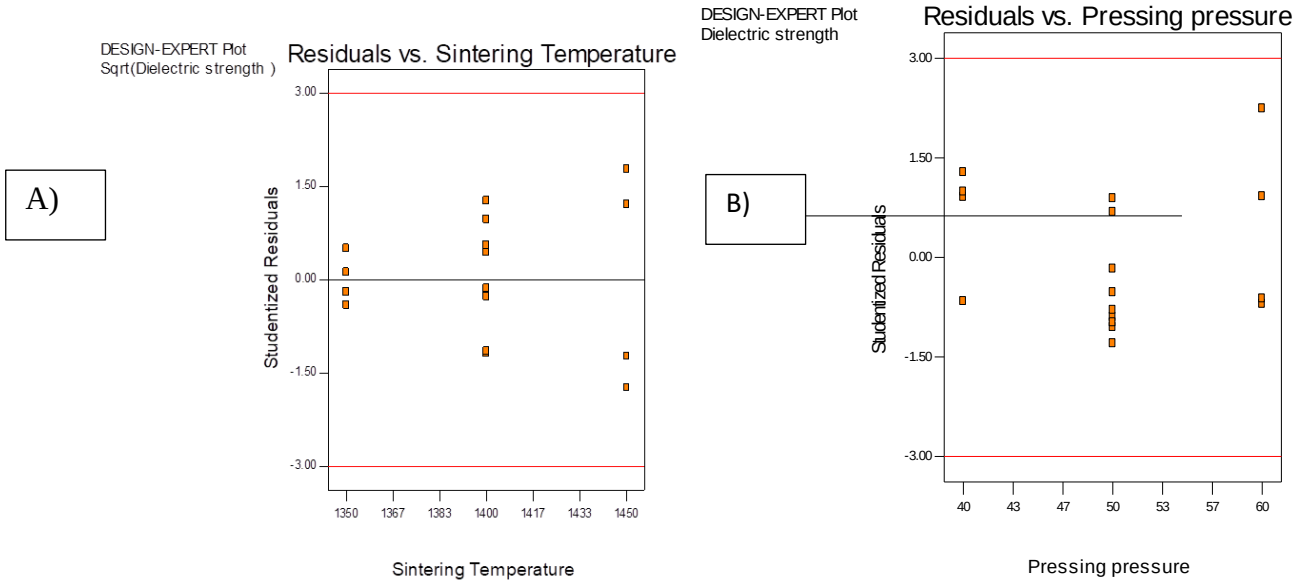

Figure4. 3 A) Residual vs. sintering temperature and B) residual vs. pressing pressure

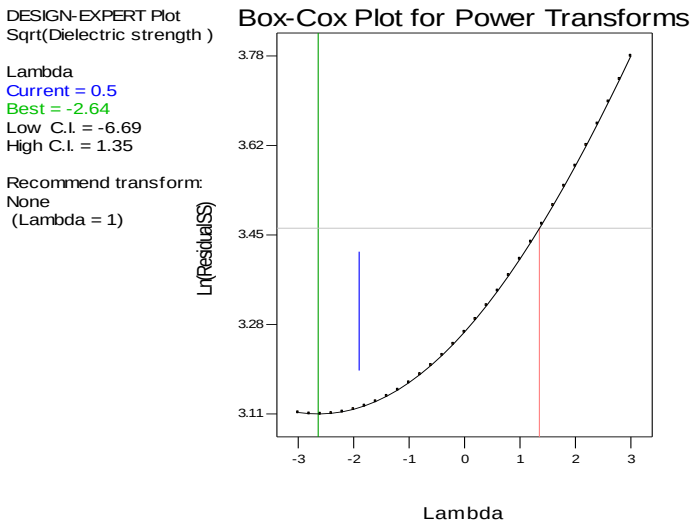

Figure4. 4 Box-Cox plot for power transforms Lambda=1 current=0.5 best=-2.64

A graph of the observed (actual) response values versus the predicted response values is observed in the figure4.5. It helps to detect observations that are not well predicted by the model.

The figure showed that the observation was well predicted by the model. In general the models are satisfactory, so possible to conclude that the empirical model is adequate to describe the dielectric strength of ceramic capacitor by response surface.

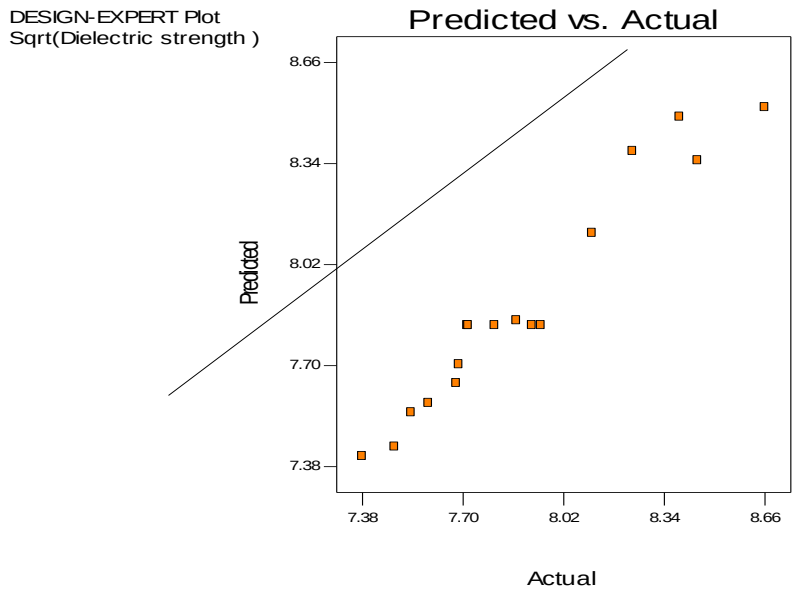

Figure4. 5 Predicted vs. actual plot of dielectric strength

4.5. Effect of Process Parameters on Dielectric Strength

4.5.1. Perturbation Plot

The perturbation plot compares the effects of all the factors at a particular point in the design space. The perturbation plot for the Dielectric strength of the ceramic material is shown in Figure 4.6. The dielectric strength response was drawn by changing only one factor over its range while the other factors were held constant. The plot demonstrates the effect of sintering temperature, pressing pressure and soaking time at a central point in the design space. The relatively flat line of pressing pressure especially soaking time shows lower effect on the dielectric strength of the ceramic capacitor. In general, with the sintering temperature increase dielectric strength of ceramic capacitor also increased, if the pressing pressure increases the dielectric strength of ceramic capacitor also increased and the soaking time increases dielectric strength of ceramic capacitor also to some extent increased.

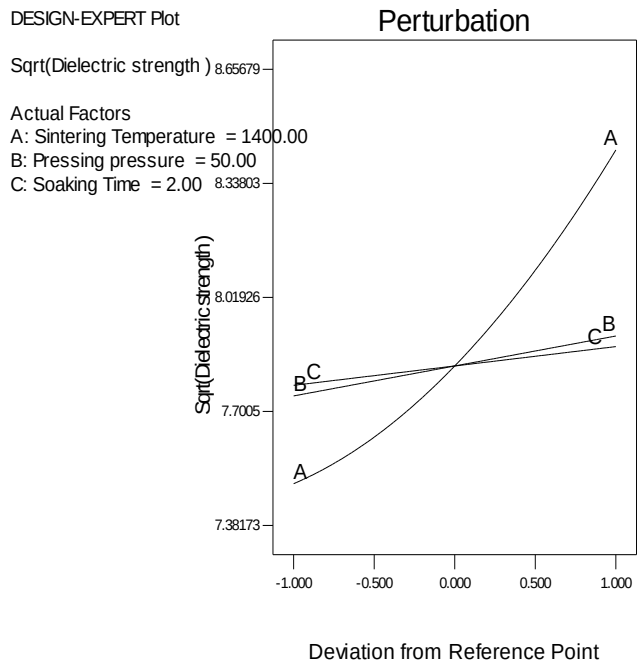

Figure4. 6 Perturbation plot for dielectric strength (A=sintering temperature, B=pressing pressure and C=soaking time)

4.5.2. One Factor Plot

One factor plot shows the effect of one factor on the dielectric strength of the ceramic capacitor. Figure4. 7one factor plots for dielectric strength (effect of sintering temperature on dielectric strength). If the sintering temperature increased the dielectric strength also increased. The one factor plot for soaking time and pressing presser the factor involved in an interaction.

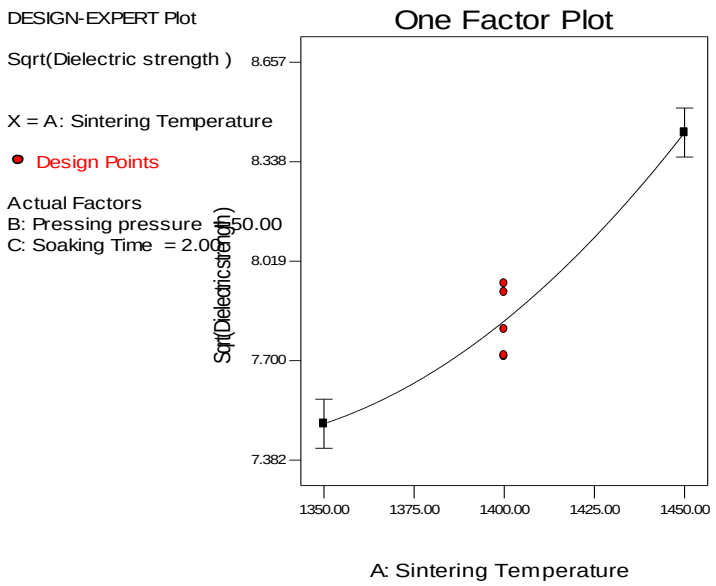

Figure4. 7 One factor plots for dielectric strength (effect of sintering temperature on dielectric strength)

4.5.3. Interaction Effects

An interaction occurs when the response is different depending on the settings of two factors. They will appear with two non-parallel lines, Figure 4.8 interaction graph of dielectric strength (X=B: pressing pressure Y=Soaking time) pressing pressure and soaking time are non-parallel indicating that the effect of one factor depends on the level of the other.

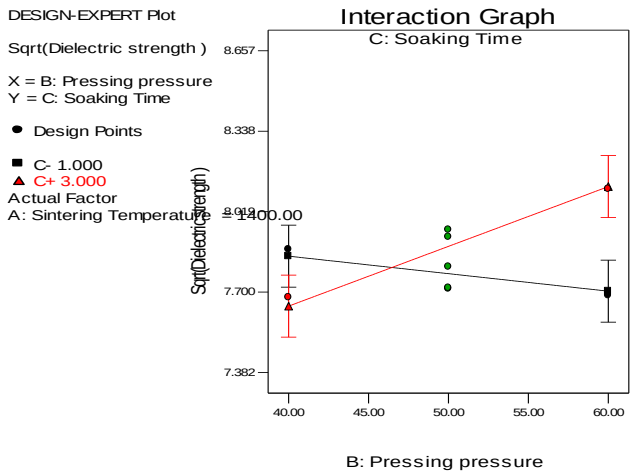

Figure4. 8 Interaction graph of dielectric strength (X=B: pressing pressure Y=Soaking time)

4.5.4. 3D Surface and contour plot for dielectric strength

The interaction effect of the factors (sintering temperature, pressing pressure and soaking time) on the dialectical strength is studied by plotting the 3D surface and contour plot. Figure4. 9 showed Three-dimensional (3D) response surface and contour plot showing the effect of sintering Temperature, Pressing Pressure and Soaking Time fixed at 2.00 Hr. A) Contour and B) 3Dsurface response respectively. As observed in the contour plot the dielectric strength is increased by increasing temperature and increasing pressure. Also the 3D plot showed that the increase of the temperature increases the dialectical strength. Other effect of contour plot and 3Dplot is presented in appendix4.

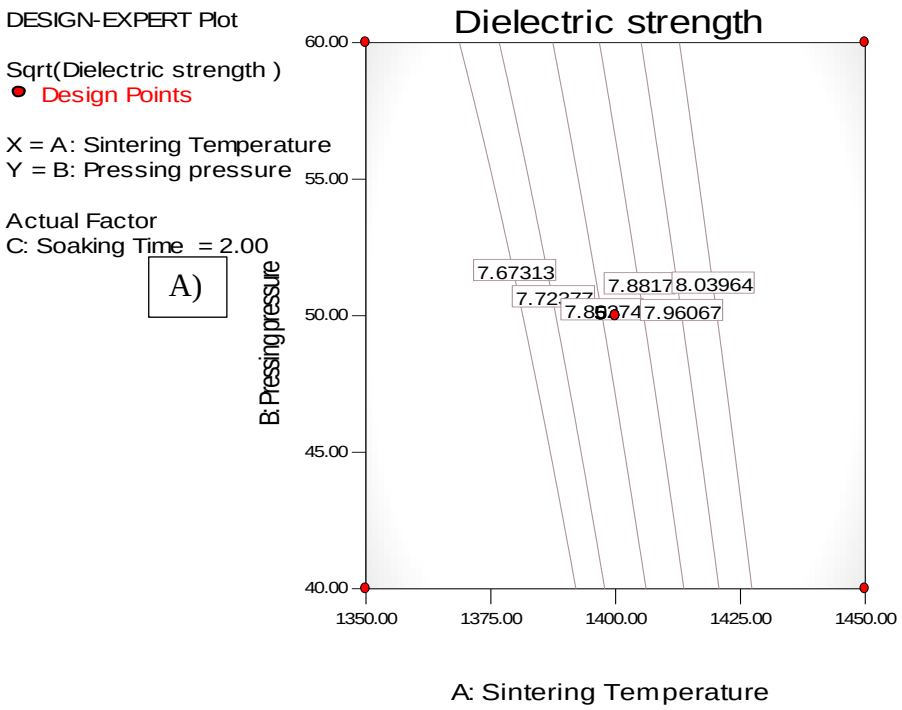

B)

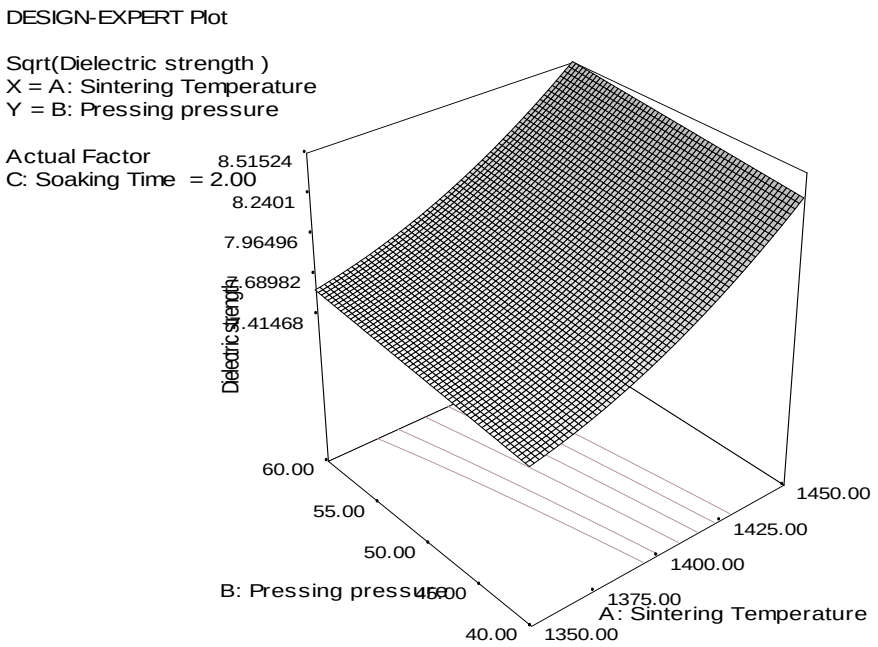

Figure4. 9 Three-dimensional 3D response surface and contour plot showing the effect of sintering Temperature, Pressing Pressure and Soaking Time fixed at 2.00 Hr. A) Contour and B) 3Dsurface response respectively.

4.6. Optimization

The aim of this study was to seek maximize the dielectric strength of ceramic capacitor in order to find the optimum process parameters. For sintering temperature the goal was in range, for pressing pressure the goal was in range, for soaking time the goal was in range. The response dielectric strength goal was maximized. The "importance" of each goal was adjusted 3 pluses (+++) the sign of 3 pluses showed that all goals to be equally important. The constraints are observed in the table4.4.

Table4. 5 Constraints to optimize the dielectric strength

Factor	Unit	Goal	Lower Limits	Upper Limits
Sintering Temperature	[°C]	Is in range	1350	1450
Pressing pressure	[Mpa]	Is in range	40	60
Soaking Time	[Hr.]	Is in range	1	3
Dielectric strength	Kv/mm	Is maximum	54.49	74.94

Figure4.10 showed that ramp plot for optimizing dielectric strength of ceramic capacitor optimume condition are fund at sintering temperature = 1449.85°c, pressing pressure=57.93MPa and soaking time=2.80hrs. , under this condition the dielectric strength of the ceamic material is 75.0135.

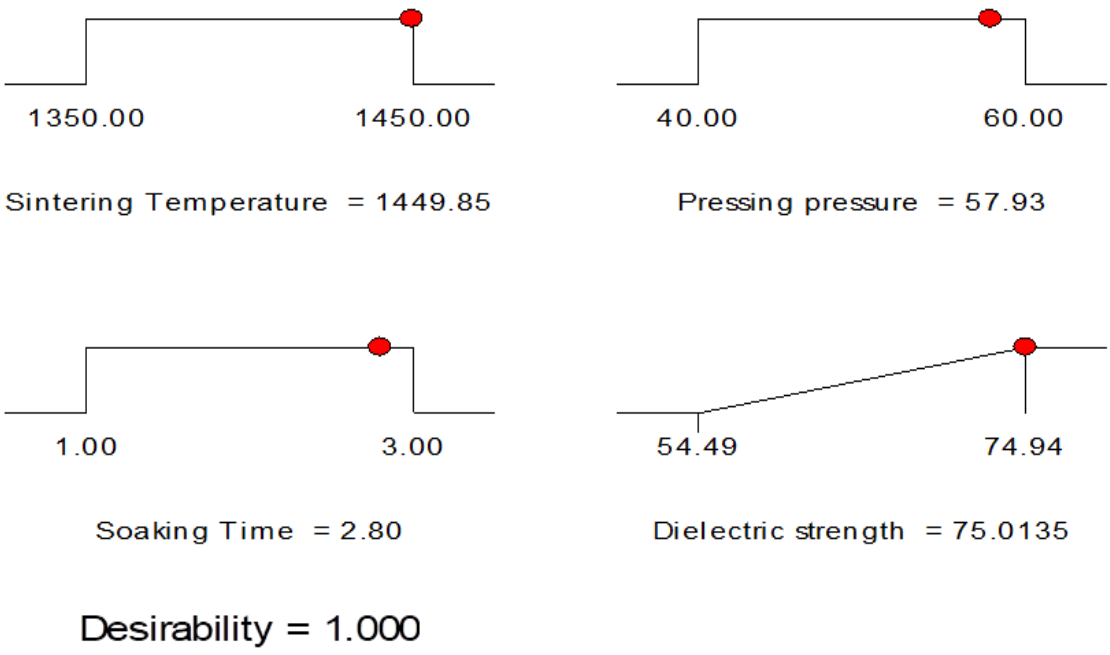

Figure4. 10 Ramp plot for optimizing dielectric strength of ceramic capacitor

Table4. 6 Other optimum conditions at different factors

Solutions Number	Sintering Temperature	Pressing pressure	Soaking Time	Dielectric strength
1	1449.85	57.93	2.80	75.0135
2	1449.84	58.52	2.96	75.7186
3	1449.74	59.98	2.55	74.9818
4	1449.96	56.62	2.98	74.9402
5	1449.40	59.14	2.70	75.0576
6	1449.40	57.75	2.97	75.2859
7	1450.00	60.00	2.22	73.9758
8	1450.00	47.21	3.00	70.7169
9	1450.00	48.89	1.69	70.6868
10	1450.00	48.11	1.29	70.4094

Figure4. 11 Show that optimum point in the Contour, 3D surface plot at each condition after adjusting the goal for sintering temperature, pressing pressure, soaking time, and the response dielectric strength. Actual factor of sintering temperature was adjusted at 1449.84.

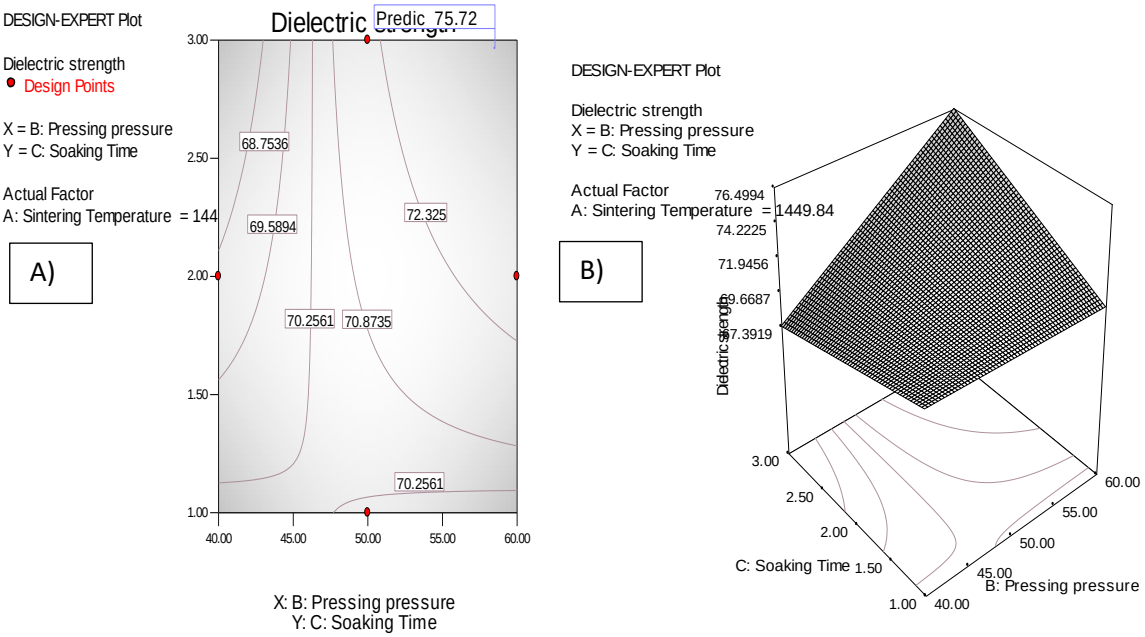

Figure4. 11 3D surface plot and contour plot for optimizing dielectric strength actual factor of sintering temperature 1449.84(A) contour plot and B) 3D surface plot)

4.7. Validation of the Developed Models

Validation of the developed model is determined whether the model accurately represents the behavior of the system or not. The developed Model was validated by comparing actual and predicted value. The actual values are calculated by the equation obtained by the design expert BBD method and the predicted values are obtained by optimizing the process. The percentages error is calculated by predicted value minus actual value divided by actual value multiply by 100. The value of percentage error was smaller values mean that close to the accepted or real value. As shown in the Table4.6 predicted and actual values of dielectric strength and percentage error presented. All values of percentage error are less than one percent this shows that the model is accurate and accepted.

Table4. 7 Predicted and actual values of dielectric strength and percentage error

Solutions Number	Sintering Temperature	Pressing pressure	Soaking Time	Dielectricstrength		percentages of error
				Predicted	Actual	
1	1449.85	57.93	2.80	75.0135	74.5717	0.59%
2	1449.84	58.52	2.96	75.7186	75.2908	0.57%
3	1449.74	59.98	2.55	74.9818	74.9330	0.065%
4	1449.96	56.62	2.98	74.9402	74.6163	0.43%
5	1449.40	59.14	2.70	75.0576	74.5524	0.68%
6	1449.40	57.75	2.97	75.2859	74.9001	0.52%
7	1450.00	60.00	2.22	73.9758	73.2768	0.95%

4.8. Mechanical Property of ceramic capacitors samples

4.8.1. Vickers hardness of ceramic capacitors samples

The hardness of the ceramic capacitors is characterized by Vickers hardness testes in Adama Science and Technology University, in department of material engineering. A diamond pyramid was pressed against the ceramic capacitor pieces with a certain normal load and the hardness was calculated based on the imprint left on the surface. Before the Vickers hardness was measured tester was adjusted at tester state: the test force at 10KgF, magnification at 20XA and time at 7s.square-based pyramid indenter whose opposite sides meet at the apex at an angle of 136° was employed in Vickers hardness test. The unit of hardness given by the test is known as the Vickers Pyramid Number (HV) or Diamond Pyramid Hardness (DPH). The hardness of ceramic capacitor is increased as the temperature, pressing pressure and soaking time increased[27]. The unit of Vickers Pyramid Number (HV) is in the form of kgf/mm^2. The figures showed in figure4.12 and figure4.13 that the temperature is the same at 1450 and the soaking time also the same at 2:00 hr. figure4.12 Vickers Pyramid Number (HV) is 425.9kgf/mm^2 and figure4.13 Vickers Pyramid Number (HV) is 399.0kgf/mm^2, this value showed that the hardness of the ceramic capacitor is increased by increasing pressure. At figure 4.13 the pressing pressure is 60 MPa and at figure 4.14 the pressing pressure is 40.

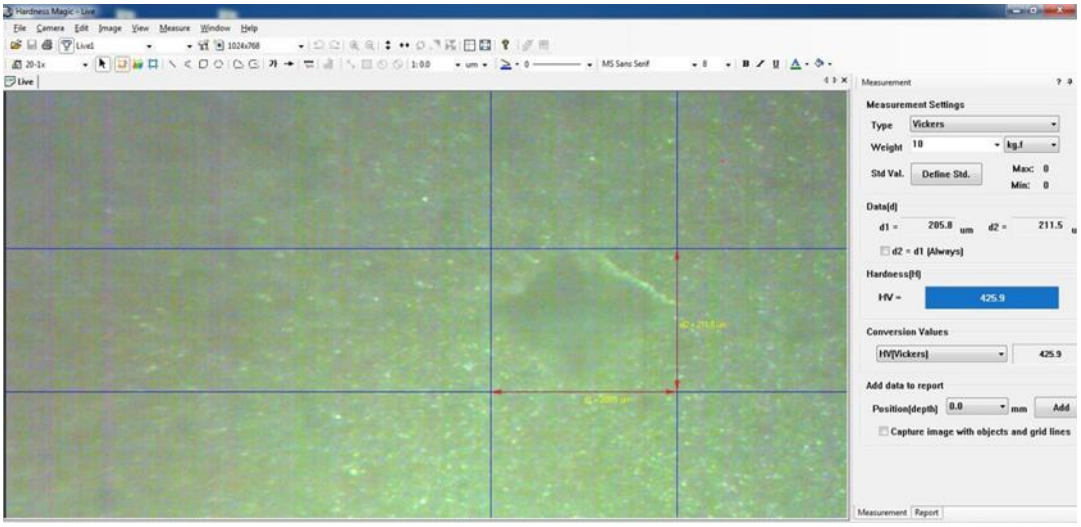

Figure4. 12 Micro Vickers hardness test set-up at a temperature of 1450, pressing pressure 60 and soaking time 2 hour (Adama science and technology university in a material engineering lab, Ethiopia)

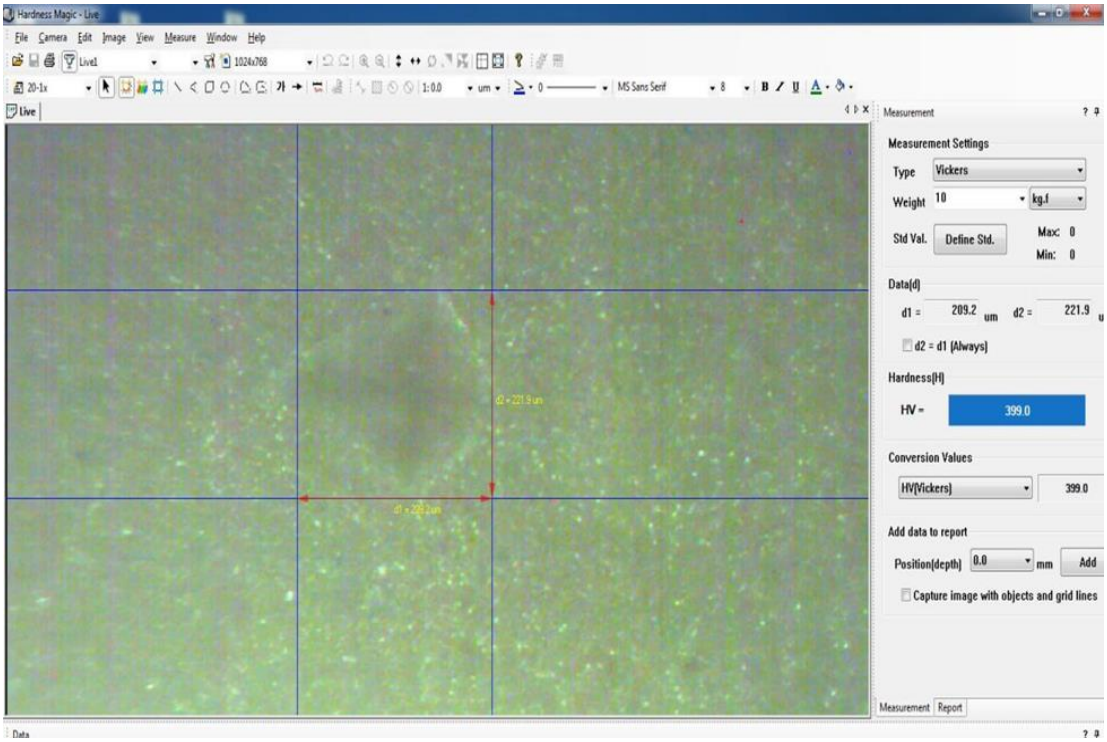

Figure4. 13 Micro Vickers hardness test set-up at a temperature of 1450, pressing pressure 40 and soaking time 2 hour (Adama science and technology university in a material engineering lab, Ethiopia)

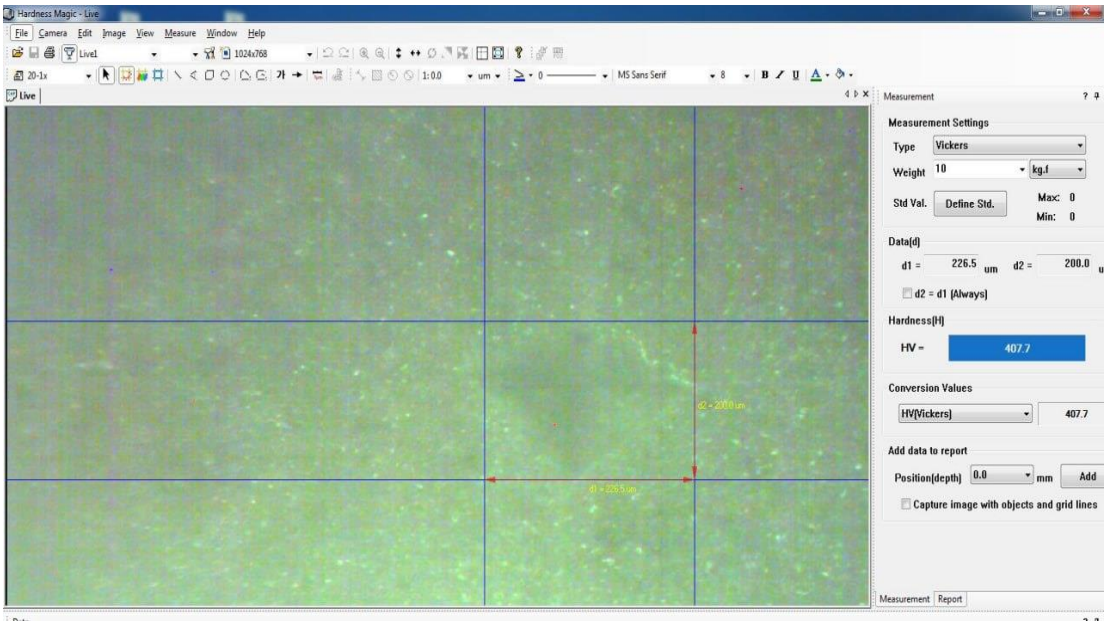

Figure4. 14 Micro Vickers hardness test set-up at a temperature of 1450, pressing pressure 50 and soaking time 3 hour (Adama science and technology university in a material engineering lab, Ethiopia)

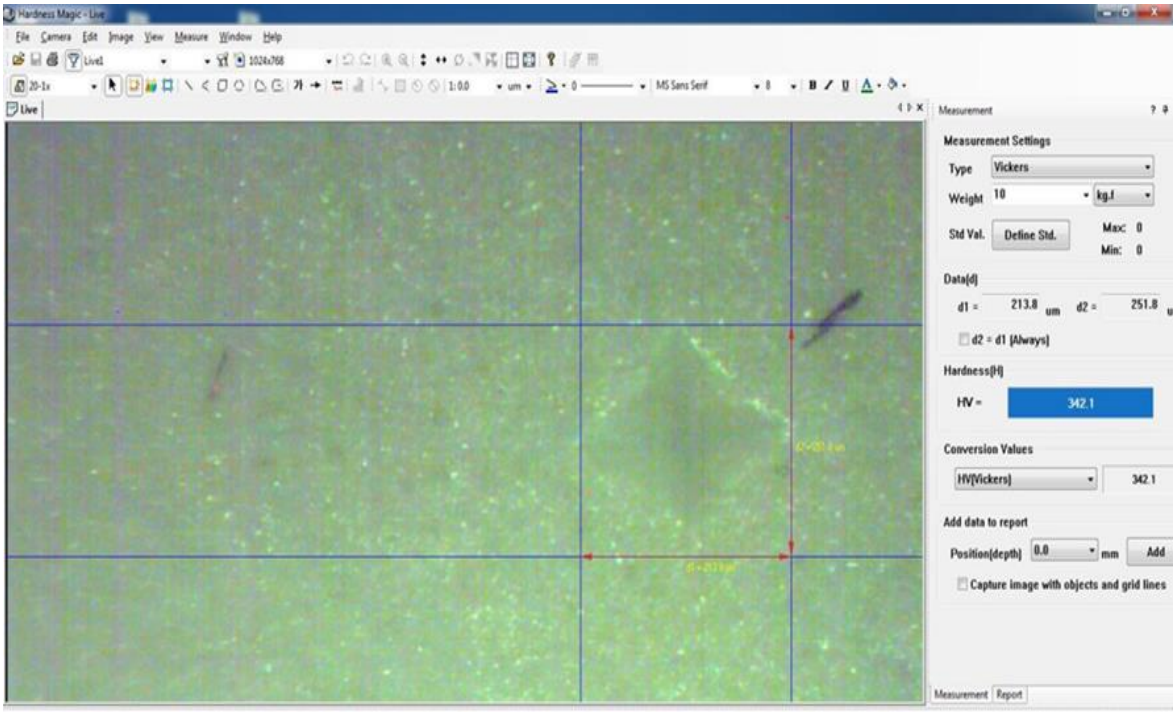

Figure4. 15 Micro Vickers hardness test set-up at a temperature of 1350, pressing pressure 50 and soaking time 3 hour (Adama science and technology university in a material engineering lab, Ethiopia)

The figure showed in the above figure4.14 and figure4.15 that the temperature is different, the pressing pressure is the same at 50 KPa and the soaking time also the same at 3:00 hr. figure4.13 Vickers Pyramid Number (HV) is 407.7kgf/mm^2 and figure4.15 Vickers Pyramid Number (HV) is 342.1kgf/mm^2, this value showed that the Vickers hardness of the ceramic capacitor is increased by increasing temperature. At figure 4.14 the sintering temperature is 1450˚C and at figure 4.15 the sintering temperature is at 1350˚C. The ceramic capacitor of the samples ware shows higher Vickers pyramid number (HV) with increasing temperature. And the pressing pressures of the ceramic capacitor also have effects; the increasing of pressing pressure increases the hardness of the material.

4.9. Physical Properties of Ceramic Capacitors Samples

4.9.1. Bulk Density of Ceramic Capacitor analysis

The illustration showed that the increase in the bulk density of the ceramic capacitor samples as firing temperature increases. The Bulk Density has inverse relation with apparent porosity and water absorption, therefore this result is expected. The Bulk Density of the ceramic capacitor sample increased as the pressing pressure and soaking time is increased. As shown in the figure4. 16, figurer 4.17 and figurer 4.18 the bulk density of the sample is increased as the pressing pressure, soaking time and sintering temperature is increased especially the sintering temperature have high effects. This is consistent with other works[27].

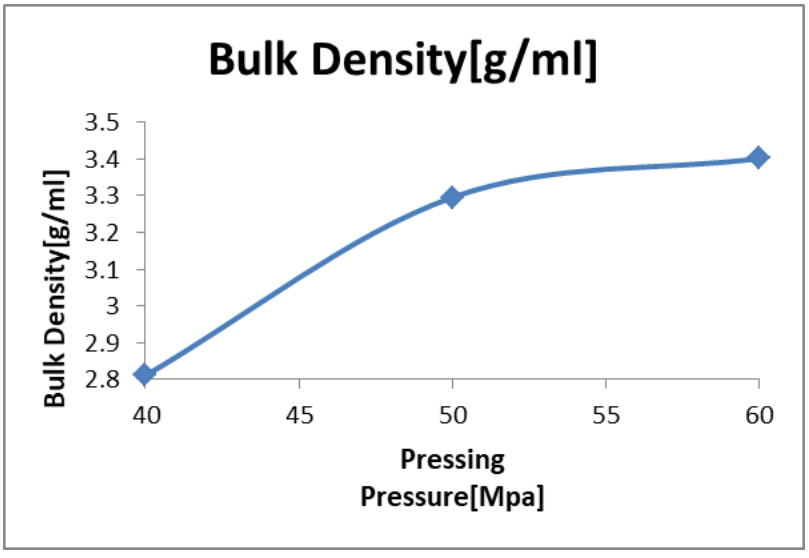

Figure4. 16 Bulk Density (g/ml) of the ceramic sample as a function of pressing pressure

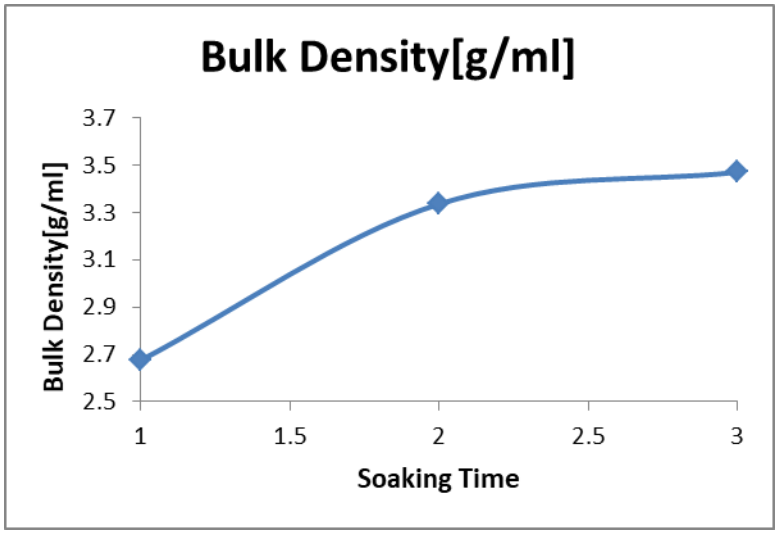

Figure4. 17 Bulk Density (g/ml) of the ceramic sample as a function of soaking time

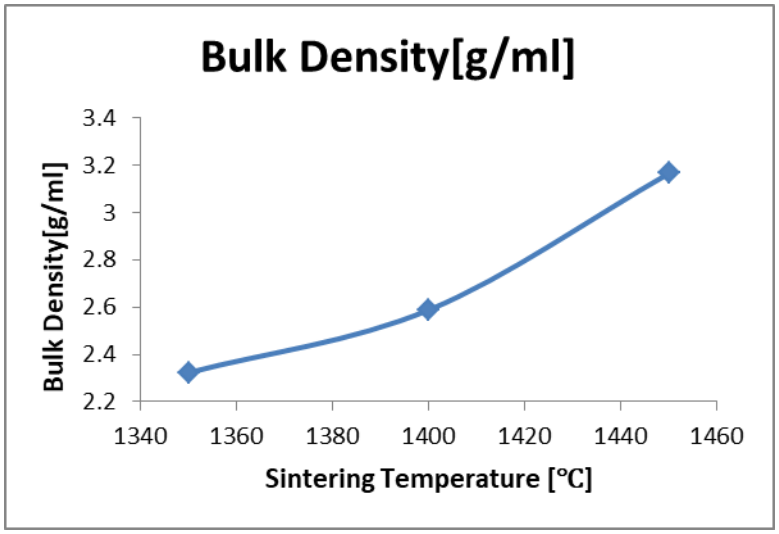

Figure4. 18 Bulk Density (g/ml) of the ceramic sample as a function of sintering temperature

4.9.2. Apparent porosity and Water absorbance of Ceramic Capacitor analysis

The physical properties of ceramic capacitor water absorption and apparent porosity of samples were decreased with increase in sintering temperature and reaching to zero as the sintering temperature increased. This could occur as a firing temperature increased the material exhibit melting resulting in liquid or glassy phase which fills the gaps or voids in the microstructure and lead to densification of the body[27].

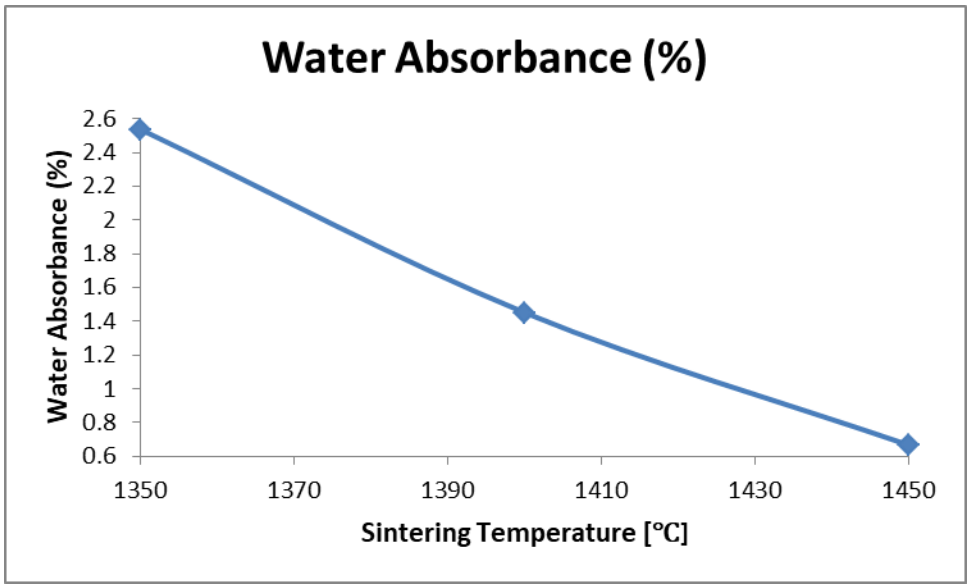

Figure4. 19 Water Absorbance of the ceramic capacitor sample as a function of sintering temperature

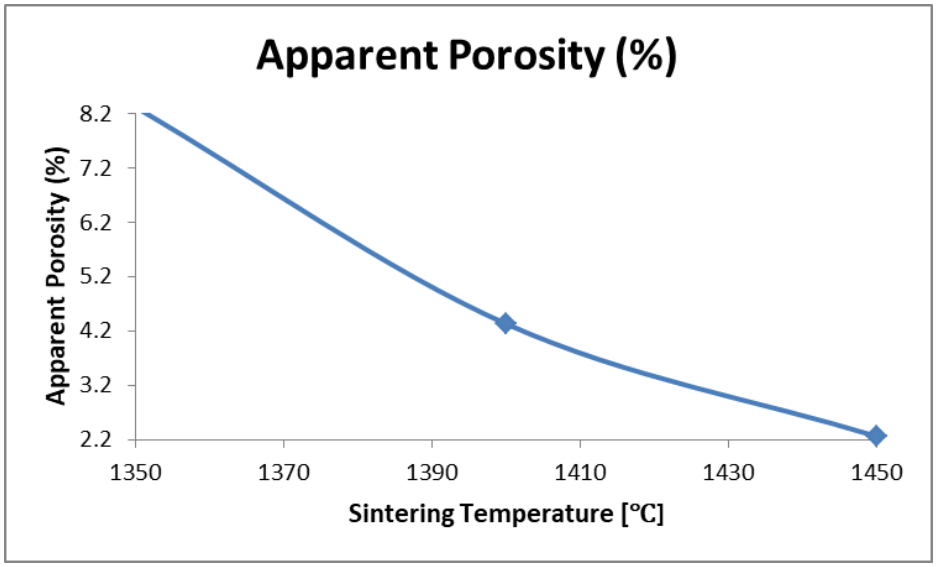

Figure4. 20 Apparent Porosity of the ceramic capacitor sample as a function of sintering temperature

As shown in the figure4. 19 and figure4. 20 the increase in sintering temperature is the decrease in Apparent Porosity and Water Absorbance. And also the decrease in Apparent Porosity and Water Absorbance as the pressing pressure increased and soaking time increased.

4.9.3. Linear Shrinkage of Ceramic Capacitor Analysis

The linear shrinkages of ceramic capacitor samples increase with increase in sintering temperature[27]. As shown in the figurer 4.21, figurer 4.22, figurer 4.23 the ceramic capacitor of the sample is increased as the sintered temperature increased, and also the pressing pressure and soaking time increased the linear of the ceramic capacitor sample were increased.

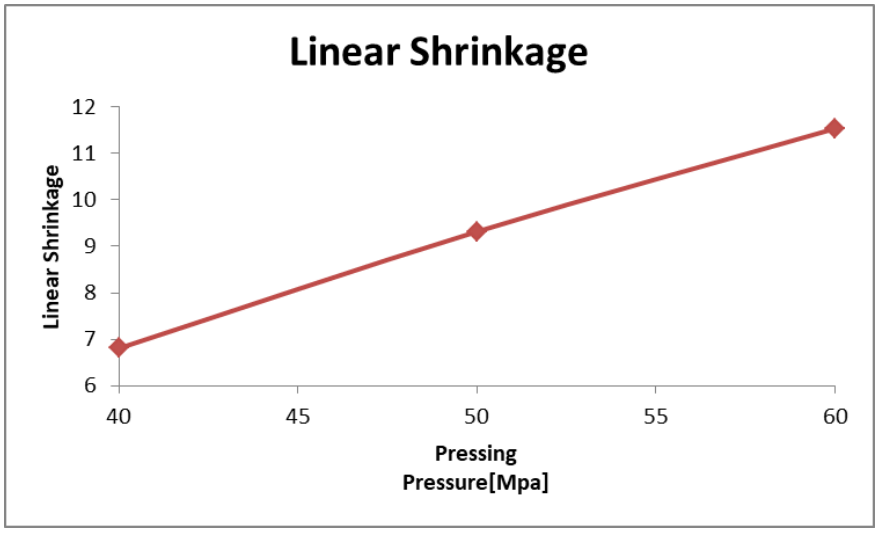

Figure4. 21 Linear shrinkage of ceramic capacitor sample as function of pressing pressure

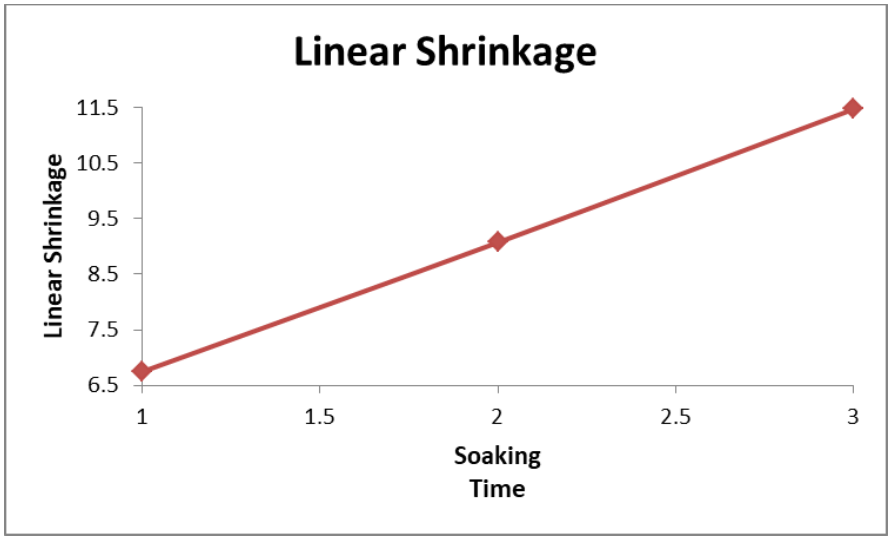

Figure4. 22 Linear shrinkage of ceramic capacitor sample as function of soaking time

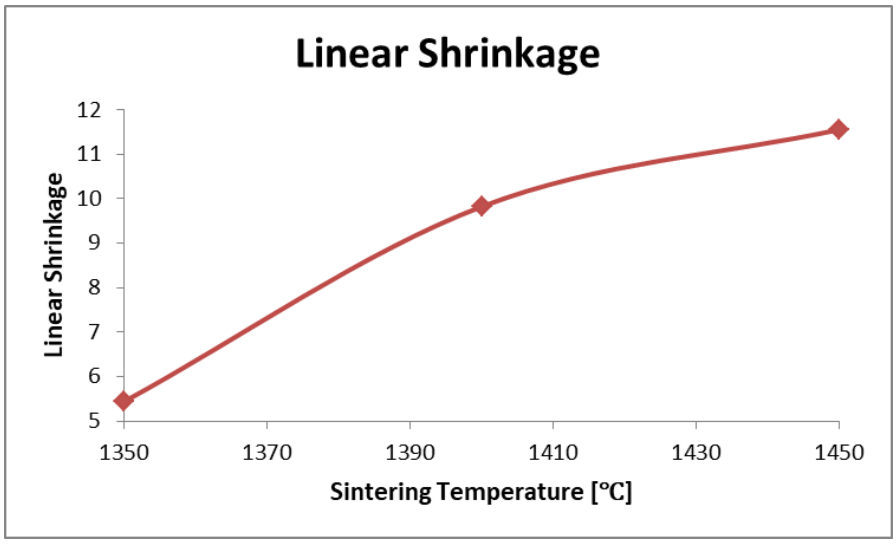

Figure4. 23 Linear shrinkage of ceramic capacitor sample as function of sintering temperature

4.10. X-ray Diffraction (XRD) Analysis

The X-ray Diffraction (XRD) Analysis was observed under different condition. divergence slit, scatter slit at 1(deg) and receiving slit 0.30000 (mm) Scanning is taken at drive axis Theta-2Theta and scan range between 10.000 - 80.000 the mode of the scanning were continuous at the speed of 3 (deg/min) with preset time 0.40 (sec). Figure4. 19 shows the XRD patterns of ceramic capacitor samples fired at 1400° C. The peaks of the XRD pattern play a vital role in the identification of the phases as well as the properties of the nanoparticles. In this case, the powders with 1400° C calcination temperature, the powders were fired for 2 hours. The results show that the samples at calcination temperature of 1400° C have sharp and narrow peaks refer to a good crystallinity.

At a calcination temperature of 1400 ^{o} C the diffraction peaks can be attributed to ZrO_2 and the $ZrTi_2O_6$ phase with some weak peaks of TiO_2 phase. At this temperature, $BaCO_3$ phase disappeared completely. As appeared in Figure4.19, it can be seen that the diffraction peaks are extended gradually at a temperature of 1400 ^{o} C. This phenomenon suggests that the tetragonal structure of the $ZrTi_2O_6$ stage is formed well at the higher calcination temperature.

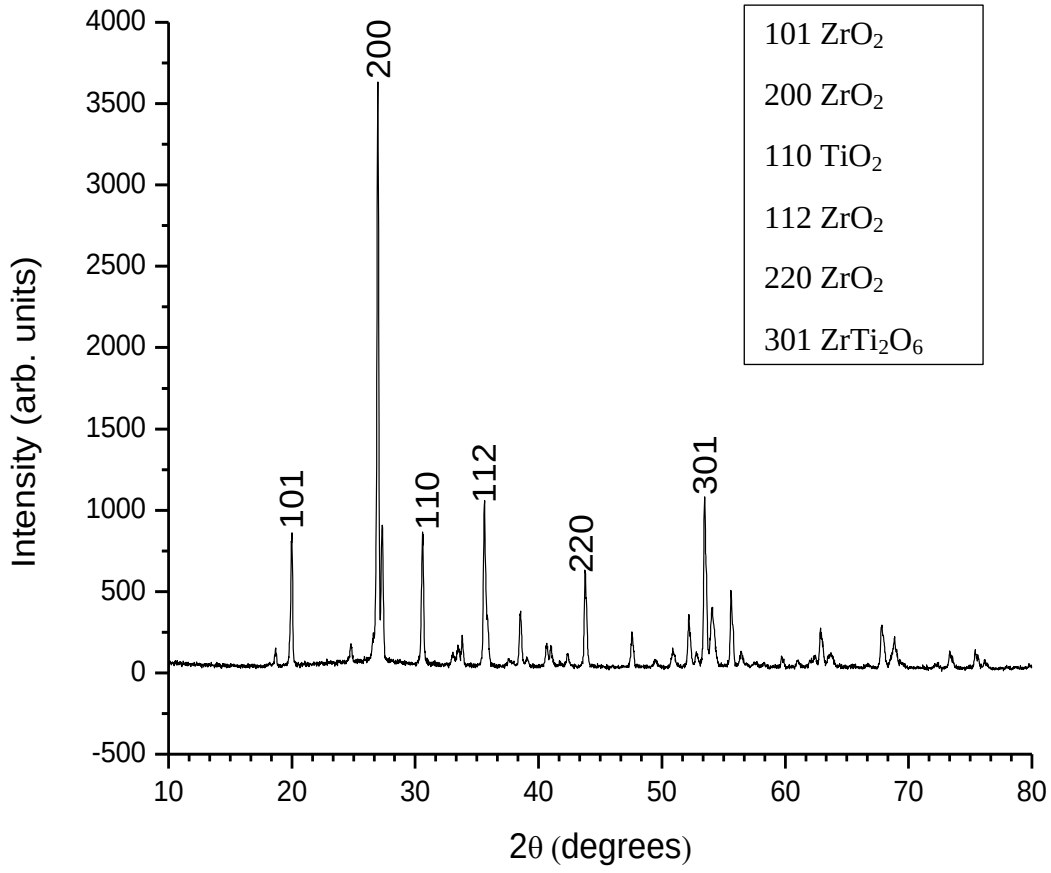

..

Figure4. 24 Powder X-ray diffraction pattern of ceramic capacitor at sintering temperature of 1400°c

The XRD results of the composition of the ceramic capacitors are weight based on the proportion and the weighted sample were sintered at a temperature of 1400°**c** and then mineralogical composition were determined by X-ray diffraction (XRD). The X-ray diffractogram of the sample shows a completely clear structure with an amorphous structure. This is consistent with the amorphous phase being constituted of network-forming in other works[28][29]. In the XRD diffraction pattern Zirconium titanate (Zr, Ti) O_2, the intermediate compound of the ZrO_2–TiO_2 system $ZrTi_2O_6$ (srilankite) are formed.

CHAPTER FIVE

5. CONCLUSION AND RECOMMENDATION

5.1. Conclusion

The present study stated that Ethiopia has mineral deposits, for this work Bentonite and clay were collected from Amhara region, North Shewa zone. The Clay sample were collected from Ankober woreda specially in Mehal Wonz and Bentonite clay collected from Merabete Woreda specially in Jemma River. The experiment was carried out by weighing the raw material based on the composition. The green body of the sample molded by dry pressing method at different pressing pressure of 40MPa, 50MPa and 60MPa and the molded sample dried by forced convection drying oven at a temperature of 100 ℃ overnight. The dried sample was sintered at different sintering temperature of 1350 ℃, 1400 ℃ and 1450 ℃ for different soaking time of 1, 2 and 3hrs and 5℃/minute firing rate. The specimen was characterized in terms of physical, mechanical and electrical properties. In general the following conclusion was drawn.

- In the present study BBD method were used to investigate the effect of sintering temperature, pressing pressure and soaking time on the dielectric strength of the sample. The order is 2FI and the model selected is polynomial.
- The dielectric strength of the ceramic capacitor increased with the increasing of sintering temperature, pressing pressure and soaking tine.
- ANOVA results showed that the effect of sintering temperature had had high influence for the dielectric strength of the ceramic capacitor. Pred R-squared 0.8889 Adj R-squared 0.9225 the difference is 0.0336 this is less than 0.2. The model provides good predictions Adeq Precision18.335 is greater than 4. The R-squared (R^2) 0.9467 indicate the model greatly fit the data. R^2 value > 0.75 indicates the suitability of the model.
- Optimum process parameters to optimize the dielectric strength of ceramic capacitor sample at a condition of sintering temperature= 1449.85, pressing pressure=57.93MPa and soaking time=2.80hrs.
- In general the ceramic capacitor can be produced by using Geominerals (Clay and Bentonite) those are available in Ethiopia, Amhara region of North Shewa.

5.2. Recommendation

This study has confirmed that there is potential in Ethiopia to produce quality ceramic capacitor using locally available raw materials for domestic demand in Ethiopia. This work focused on the production and characterization of the ceramic capacitor made from raw materials that are available in North Shewa Zone, Ethiopia, and Metal Oxides.

From this work, the following are the recommendations;

- A result of the present study has demonstrated the probability of producing good quality ceramic capacitor from locally available geo-materials. Subsequently, nearby accessible geo-minerals can be investigated for huge scale generation of ceramic capacitor.
- It need further study in order to achieve the high quality ceramic capacitor, in Ethiopia as the studies made so far this area is limited.
- The microstructure of Ceramic Capacitor was not measured in this work due to the inaccessibility of a scanning electron microscope (SEM); therefore, the morphology of the ceramic capacitor should be studied further.
- The microstructure of Ceramic Capacitor at a condition of sintering temperature= 1449.85, pressing pressure=57.93MPa and soaking time=2.80hrs. Was not measured by using XRD. Therefore, the morphology of the ceramic capacitor at optimum process parameters should be studied further.

REFERENCES

[1] J. Ho, T. R. Jow, and S. Boggs, "Historical introduction to capacitor technology," *IEEE Electr. Insul. Mag.*, vol. 26, no. 1, pp. 20–25, 2010, doi: 10.1109/MEI.2010.5383924.

[2] M. P. Pechini, "Method of Pre Parng Lead and Alkalne Earth Titanates and Nobates and Coat.," *US Pat. 3,330,697*, p. 2, 1967.

[3] T. Pradell and J. Molera, "Ceramic technology. How to characterise ceramic glazes," *Archaeol. Anthropol. Sci.*, vol. 12, no. 8, pp. 0–2, 2020, doi: 10.1007/s12520-020-01136-9.

[4] M. J. Pan and C. Randall, "A brief introduction to ceramic capacitors," *IEEE Electr. Insul. Mag.*, vol. 26, no. 3, pp. 44–50, 2010, doi: 10.1109/MEI.2010.5482787.

[5] S. M. Lambert, B. C. Mecrow, R. Abebe, G. Vakil, and C. M. Johnson, "Integrated Drives for Transport - A Review of the Enabling Thermal Management Technology," *2015 IEEE Veh. Power Propuls. Conf. VPPC 2015 - Proc.*, 2015, doi: 10.1109/VPPC.2015.7352968.

[6] M. El Khalloufi, O. Drevelle, and G. Soucy, "Titanium: An overview of resources and production methods," *Minerals*, vol. 11, no. 12, 2021, doi: 10.3390/min11121425.

[7] H. Maros and S. Juniar, "Influence of the BaTiO3 addition to K0.5Na0.5NbO3 lead-free ceramics on the vacancy-like defect structure and dielectric properties, ," pp. 1–23, 2016.

[8] C. G. P. Moraes *et al.*, "Investigating the Correlation between the Microstructure and Electrical Properties of FeSbO4 Ceramics," *Materials (Basel).*, vol. 15, no. 19, 2022, doi: 10.3390/ma15196555.

[9] Q. Li, "Titanium Dioxide Dielectric Layers Made By Anodization of Titanium: the Effect of Dissolved Nitrogen and Oxygen," pp. 1–102, 2013.

[10] T. Manfredini and M. Hanuskova, "Natural raw materials in 'Traditional' ceramic manufacturing," *J. Univ. Chem. Technol. Metall.*, vol. 47, no. 4, pp. 465–470, 2012.

[11] A. O. Surendranathan, "An Introduction to Ceramics and Refractories," *An Introduction to Ceramics and Refractories*. 2014, doi: 10.1201/b17811.

[12] J. Thammapreecha, A. Treetong, B. Putasaeng, N.Witit-anun, S. Chaiyakun, and P.

Limsuwan, "Dielectric Properties of ZrTiO4 Thin Films Prepared by Reactive DC Magnetron Co-sputtering," *J. Phys. Sci. Appl.*, vol. 7, no. 6, pp. 24–29, 2017, doi: 10.17265/2159-5348/2017.06.004.

[13] J. O. Ohimai, P. Ohimai, and H. Sado, "The divergent use of contemporary ceramics in engineering," vol. 17, no. 1, pp. 1–7, 2010.

[14] S. Jang, S. Park, and C. jun Bae, "Development of ceramic additive manufacturing: process and materials technology," *Biomed. Eng. Lett.*, vol. 10, no. 4, pp. 493–503, 2020, doi: 10.1007/s13534-020-00175-4.

[15] L. M. Calle *et al.*, "Refractory materials for flame deflector protection," *AIAA Sp. Conf. Expo. 2010*, 2010, doi: 10.2514/6.2010-8749.

[16] E. Wuchina, E. Opila, M. Opeka, W. Fahrenholtz, and I. Talmy, "UHTCs: Ultra-High Temperature Ceramic materials for extreme environment applications," *Electrochem. Soc. Interface*, vol. 16, no. 4, pp. 30–36, 2007, doi: 10.1149/2.f04074if.

[17] P. Colomban, A. Tournie, and L. Bellot-Gurlet, "Raman identification of glassy silicates used in ceramics, glass and jewellery: A tentative differentiation guide," *J. Raman Spectrosc.*, vol. 37, no. 8, pp. 841–852, 2006, doi: 10.1002/jrs.1515.

[18] D. Kujanen, "Daniel Kujanen TECHNICAL CERAMICS AND REFRAC- TORIES APPLICATIONS AND VOLUMES," no. April, 2019.

[19] G. V. Franks, C. Tallon, A. R. Studart, M. L. Sesso, and S. Leo, "Colloidal processing: enabling complex shaped ceramics with unique multiscale structures," *J. Am. Ceram. Soc.*, vol. 100, no. 2, pp. 458–490, 2017, doi: 10.1111/jace.14705.

[20] A. Teverovsky, "Mechanical Testing of MLCCs," pp. 1–50, 2016.

[21] H. M. Lee and D. K. Kim, "High-strength AlN ceramics by low-temperature sintering with CaZrO3-Y2O3 co-additives," *J. Eur. Ceram. Soc.*, vol. 34, no. 15, pp. 3627–3633, 2014, doi: 10.1016/j.jeurceramsoc.2014.05.008.

[22] European Comission, "Ceramic Manufacturing Industry," *Eur. Comm.*, no. August, pp. 210–211, 2007.

[23] W. Conshohocken, "Standard Test Methods for Apparent Porosity , Liquid Absorption , Apparent Specific Gravity , and Bulk Density of Refractory Shapes by Vacuum," *Methods*, vol. 93, no. April 1993, pp. 1–6, 2000, doi: 10.1520/C0830-06R11.2.

[24] B. P. Kagonbé, D. Tsozué, A. N. Nzeukou, and S. Ngos III, "Mineralogical, Geochemical and Physico-Chemical Characterization of Clay Raw Materials from Three Clay Deposits in Northern Cameroon," *J. Geosci. Environ. Prot.*, vol. 09, no. 06, pp. 86–99, 2021, doi: 10.4236/gep.2021.96005.

[25] Z. Cai *et al.*, "Significantly enhanced dielectric breakdown strength and energy density of multilayer ceramic capacitors with high efficiency by electrodes structure design," *Appl. Phys. Lett.*, vol. 115, no. 2, 2019, doi: 10.1063/1.5110527.

[26] M. Letz *et al.*, "Glass ceramics as dielectrics for high power capacitors," *Proc. 2014 IEEE Int. Power Modul. High Volt. Conf. IPMHVC 2014*, pp. 1–4, 2015, doi: 10.1109/IPMHVC.2014.7287193.

[27] S. E. Bendaoudi, M. Bounazef, and A. Djeffal, "The effect of sintering temperature on the porosity and compressive strength of corundum," *J. Mech. Behav. Mater.*, vol. 27, no. 3–4, pp. 3–5, 2018, doi: 10.1515/jmbm-2018-0018.

[28] N. Y. Mostafa, A. A. Shaltout, M. S. Abdel-Aal, and A. El-maghraby, "Sintering mechanism of blast furnace slag-kaolin ceramics," *Mater. Des.*, vol. 31, no. 8, pp. 3677–3682, 2010, doi: 10.1016/j.matdes.2010.03.001.

[29] U. Troitzsch, A. G. Christy, and D. J. Ellis, "The crystal structure of disordered (Zr,Ti)O2 solid solution including srilankite: Evolution towards tetragonal ZrO2 with increasing Zr," *Phys. Chem. Miner.*, vol. 32, no. 7, pp. 504–514, 2005, doi: 10.1007/s00269-005-0027-0.

APPENDIXES

Appendix 1: The experimental result

Table A1. 1 Effect of sintering temperature on water absorbance, bulk density and apparent porosity.

Sintering Temperature [℃]	Water Absorbance (%)			Apparent Porosity (%)			Bulk Density[g/ml]		
	Trial 1	Trial 2	Average	Trial 1	Trial 2	Average	Trial 1	Trial 2	Average
1350	2.0134	3.0562	2.5348	6.5343	10.1018	8.31805	2.2213	2.4251	2.3232
1400	1.1972	1.7012	1.4492	3.1125	5.5375	4.325	2.5211	2.6567	2.5889
1450	0.5565	0.7721	0.6643	1.8553	2.6547	2.255	2.9521	3.3811	3.1666

Table A1. 2 Effect Soaking Time on water absorbance, bulk density and apparent porosity.

Soaking Time	Water Absorbance (%)			Apparent Porosity (%)			Bulk Density[g/ml]		
	Trial 1	Trial 2	Average	Trial 1	Trial 2	Average	Trial 1	Trial 2	Average
1	1.9877	3.1121	2.5499	8.8823	9.5071	9.1947	2.4543	2.8977	2.676
2	1.7871	1.7217	1.7544	5.9871	6.1233	6.0552	3.2347	3.4377	3.3362
3	0.8887	1.8719	1.3803	3.8679	4.5673	4.2176	3.4423	3.4989	3.4706

Table A1. 3 Effect Pressing Pressure on water absorbance, bulk density and apparent porosity.

Pressing Pressure[Mpa]	Water Absorbance (%)			Apparent Porosity (%)			Bulk Density[g/ml]		
	Trial 1	Trial 2	Average	Trial 1	Trial 2	Average	Trial 1	Trial 2	Average
40	2.0761	3.0611	2.5686	8.0217	10.1325	9.0771	2.6345	2.9881	2.8113
50	1.7783	1.8131	1.7957	5.2517	6.4045	5.8281	3.2508	3.3402	3.2955
60	0.8975	1.7115	1.3045	3.7448	4.4374	4.0911	3.3501	3.4525	3.4013

Table A1. 4 Water absorption of all samples.

Run order	Sintering Temperature [°C]	Pressing pressure [Mpa]	Soaking Time [Hr.]	Dry mass [gm]	Saturated mass[gm]	Suspended mass[gm]	Water absorbance (%)
1	1450	50	3.00	5.1457	5.1828	3.2297	0.7209
2	1450	40	2.00	5.1567	5.2121	3.2124	1.0743
3	1400	50	2.00	5.5339	5.5830	3.9430	0.8872
4	1400	40	1.00	5.5823	5.6421	3.5431	1.0712
5	1400	50	2.00	5.5443	5.5904	3.9504	0.8315
6	1400	60	3.00	5.6468	5.7144	4.0260	1.1971
7	1350	50	1.00	5.3347	5.4269	3.6376	1.7283
8	1350	50	3.00	5.3673	5.5316	3.9078	1.8140
9	1350	40	2.00	5.4465	5.5453	4.0027	3.0611
10	1400	50	2.00	5.5257	5.5764	3.9321	0.9175
11	1400	60	1.00	5.5624	5.5992	3.9678	0.6616
12	1400	40	3.00	5.3887	5.4809	3.8760	1.7111
13	1350	60	2.00	5.2595	5.3271	3.8037	1.2853
14	1400	50	2.00	5.2467	5.2943	3.3497	0.9072
15	1450	50	1.00	5.3482	5.3913	3.7501	0.8059
16	1450	60	2.00	5.3132	5.3421	3.7710	0.5439
17	1400	50	2.00	5.5631	5.5997	3.9567	0.6579

Table A1. 5 Apparent porosity of all sample

Run order	Sintering Temperature [°C]	Pressing pressure [Mpa]	Soaking Time [Hr.]	Dry mass [gm]	Saturated mass[gm]	Suspend-ed mass[gm]	Apparent porosi-ty[%]
1	1450	50	3.00	5.1457	5.1828	3.2297	1.8995
2	1450	40	2.00	5.1567	5.2121	3.2124	2.7704
3	1400	50	2.00	5.5339	5.5830	3.9430	2.9939
4	1400	40	1.00	5.5823	5.6421	3.5431	2.8490
5	1400	50	2.00	5.5443	5.5904	3.9504	2.8110
6	1400	60	3.00	5.6468	5.7144	4.0260	4.0038
7	1350	50	1.00	5.3347	5.4269	3.6376	5.1528
8	1350	50	3.00	5.3673	5.5316	3.9078	6.4048
9	1350	40	2.00	5.4465	5.5453	4.0027	10.1182
10	1400	50	2.00	5.5257	5.5764	3.9321	3.0834
11	1400	60	1.00	5.5624	5.5992	3.9678	2.2557
12	1400	40	3.00	5.3887	5.4809	3.8760	5.7449
13	1350	60	2.00	5.2595	5.3271	3.8037	4.4374
14	1400	50	2.00	5.2467	5.2943	3.3497	2.4478
15	1450	50	1.00	5.3482	5.3913	3.7501	2.6261
16	1450	60	2.00	5.3132	5.3421	3.7710	1.8395
17	1400	50	2.00	5.5631	5.5997	3.9567	2.2276

Table A1. 6 Bulk density data of all samples.

Run order	Sintering Temperature [°C]	Pressing pressure [Mpa]	Soaking Time [Hr.]	Dry mass [gm]	Saturated mass[gm]	Suspend-ed mass[gm]	Bulk density [g/ml]
1	1450	50	3.00	5.1457	5.1828	3.2297	2.6346
2	1450	40	2.00	5.1567	5.2121	3.2124	2.5787
3	1400	50	2.00	5.5339	5.5830	3.9430	3.3743
4	1400	40	1.00	5.5823	5.6421	3.5431	2.6595
5	1400	50	2.00	5.5443	5.5904	3.9504	3.3807
6	1400	60	3.00	5.6468	5.7144	4.0260	3.3445
7	1350	50	1.00	5.3347	5.4269	3.6376	2.9814
8	1350	50	3.00	5.3673	5.5316	3.9078	3.5307
9	1350	40	2.00	5.4465	5.5453	4.0027	3.3054
10	1400	50	2.00	5.5257	5.5764	3.9321	3.3605
11	1400	60	1.00	5.5624	5.5992	3.9678	3.4096
12	1400	40	3.00	5.3887	5.4809	3.8760	3.3576
13	1350	60	2.00	5.2595	5.3271	3.8037	3.4525
14	1400	50	2.00	5.2467	5.2943	3.3497	2.6981
15	1450	50	1.00	5.3482	5.3913	3.7501	3.2587
16	1450	60	2.00	5.3132	5.3421	3.7710	3.3818
17	1400	50	2.00	5.5631	5.5997	3.9567	3.3859

Table A1. 7 Effect of pressing pressure on linear shrinkage

Pressing Pressure[Mpa]	Linear Shrinkage		
	Trial 1	Trial 2	Average
40	6.7264	6.8834	6.8049
50	8.7892	9.8453	9.3173
60	10.2896	12.7784	11.534

Table A1. 8 Effect of sintering temperature on linear shrinkage

Sintering Temperature [°C]	Linear Shrinkage		
	Trial 1	Trial 2	Average
1350	5.1198	5.7662	5.442
1400	9.7441	9.9113	9.8277
1450	10.3133	12.8023	11.5578

Table A1. 9 Effect of soaking time on linear shrinkage

Soaking Time	Linear Shrinkage		
	Trial 1	Trial 2	Average
1	6.6176	6.8702	6.7439
2	8.4012	9.7444	9.0728
3	10.2432	12.7032	11.4732

Table A1. 10 Linear shrinkage data of all samples

Run order	Sintering Temperature [°C]	Pressing pressure [Mpa]	Soaking Time [Hr.]	dry length (Before sintering) [mm]	fired length (After sintering) [mm]	linear Shrinkage
1	1450	50	3.00	4.9882	4.3452	12.890
2	1450	40	2.00	4.9124	4.4634	9.1140
3	1400	50	2.00	4.8941	4.4823	8.4142
4	1400	40	1.00	4.9764	4.4915	9.7440
5	1400	50	2.00	4.9882	4.4767	10.2542
6	1400	60	3.00	4.8771	4.4672	8.4046
7	1350	50	1.00	4.9423	4.6583	5.7463
8	1350	50	3.00	4.9567	4.6287	6.6173
9	1350	40	2.00	4.9365	4.6812	5.1717
10	1400	50	2.00	4.8825	4.4231	9.4091
11	1400	60	1.00	4.9224	4.4474	9.6498
12	1400	40	3.00	4.8789	4.5126	7.5078
13	1350	60	2.00	4.8984	4.6481	5.1098
14	1400	50	2.00	4.9554	4.4716	9.7631
15	1450	50	1.00	4.9665	4.4538	10.3232
16	1450	60	2.00	4.9913	4.3523	12.8023
17	1400	50	2.00	4.9621	4.4987	9.3388

Table A1. 11 Result of all Dielectric strength [KV/mm] data

Run order	Sintering Temperature [°C]	Pressing pressure [Mpa]	Soaking Time [Hr.]	fired length (After sintering) [mm]	Break down voltage (Kv)	Dielectric strength [KV/mm]
1	1450	50	3.00	4.35	306	70.34
2	1450	40	2.00	4.46	318	71.30
3	1400	50	2.00	4.48	281	62.72
4	1400	40	1.00	4.49	278	61.92
5	1400	50	2.00	4.48	283	63.17
6	1400	60	3.00	4.47	294	65.77
7	1350	50	1.00	4.66	261	56.01
8	1350	50	3.00	4.63	263	56.80
9	1350	40	2.00	4.68	255	54.49
10	1400	50	2.00	4.42	269	60.86
11	1400	60	1.00	4.45	263	59.10
12	1400	40	3.00	4.51	266	58.98
13	1350	60	2.00	4.65	268	57.63
14	1400	50	2.00	4.47	266	59.51
15	1450	50	1.00	4.45	302	67.87
16	1450	60	2.00	4.35	326	74.94
17	1400	50	2.00	4.50	268	59.56

Table A1. 12 Vickers Hardness (MPa) and tensile strength (MPa) of all data.

Run order	Sintering Temperature [℃]	Pressing pressure [Mpa]	Soaking Time [Hr.]	Vickers Hardness (KgF/mm^2)	Vickers Hardness (MPa)	tensile strength (MPa)
1	1450	50	3.00	407.7	3998	1332.7
2	1450	40	2.00	399	3913	1304.3
3	1400	50	2.00	378.6	3713	1237.7
4	1400	40	1.00	360.4	3534	1178.0
5	1400	50	2.00	378.5	3712	1237.3
6	1400	60	3.00	382.5	3751	1250.3
7	1350	50	1.00	335.5	3290	1096.7
8	1350	50	3.00	342.1	3355	1118.3
9	1350	40	2.00	329	3227	1075.7
10	1400	50	2.00	376.6	3693	1231.0
11	1400	60	1.00	380.6	3733	1244.3
12	1400	40	3.00	365.4	3583	1194.3
13	1350	60	2.00	354.3	3475	1158.3
14	1400	50	2.00	370.8	3636	1212.0
15	1450	50	1.00	401.2	3935	1311.7
16	1450	60	2.00	425.9	4177	1392.3
17	1400	50	2.00	374.7	3675	1225.0

Appendix 2: Sequential Model and fit Summary Statistics

Design Summary

Study Type	Response Surface	**Experiments**	17
Initial Design	Box Behnken	**Blocks**	No Blocks
Design Model	Quadratic		

Response	Name	Units	Obs	Minimum	Maximum	Trans	Model
Y1	Dielectric strength	KV/mm	17	54.49	74.94	Square root	RQuadratic

Factor	Name	Units	Type	Low Actual	High Actual	Low Coded	High Coded
A	Sintering Temperature	Degree centigrade	Numeric	1350.00	1450.00	-1.000	1.000
B	Pressing pressure	Mpa	Numeric	40.00	60.00	-1.000	1.000
C	Soaking Time	Hr.	Numeric	1.00	3.00	-1.000	1.000

Order: 2FI model: Polynomial

3 Factors: A, B, C

Design Matrix Evaluation for Response Surface 2FI Model

No aliases found for 2FI Model

Degrees of Freedom for Evaluation

Model	6
Residuals	10
Lack 0f Fit	*6*
Pure Error	*4*
Corr Total	16

Term	StdErr**	VIF	Ri-Squared	Power at 5 % alpha level for effect of 1/2 Std. Dev.	1 Std. Dev.	2 Std. Dev.
A	0.35	1.00	0.0000	9.8 %	24.9 %	72.2 %
B	0.35	1.00	0.0000	9.8 %	24.9 %	72.2%
C	0.35	1.00	0.0000	9.8 %	24.9 %	72.2%
AB	0.50	1.00	0.0000	7.4 %	14.8 %	44.0%
AC	0.50	1.00	0.0000	7.4 %	14.8 %	44.0%
BC	0.50	1.00	0.0000	7.4 %	14.8 %	44.0%

**Basis Std. Dev. = 1.0

Transformation: none because response ranges from 54.49 to 74.94. Ratio of max to min is 1.3753. A ratio greater than 10 usually indicates a transformation is required. For ratios less than 3 the power transforms have little effect. But for this work Square root is selected.

Sequential Model Sum of Squares

Source	Sum of Squares	DF	Mean Square	F Value	Prob > F	
Mean	1058.88	1	1058.88			
Linear	1.82	3	0.61	27.58	< 0.0001	Suggested
2FI	0.096	3	0.032	1.69	0.2323	
Quadratic	0.10	3	0.034	2.79	0.1188	
Cubic	0.038	3	0.013	1.05	0.4616	Aliased
Residual	0.048	4	0.012			
Total	1060.99	17	62.41			

"Sequential Model Sum of Squares": Select the highest order polynomial where the additional terms are significant and the model is not aliased.

Lack of Fit Tests

Lack of Fit Tests

Source	Sum of Squares	DF	Mean Square	F Value	Prob > F	
Linear	0.24	9	0.026	2.19	0.2346	Suggested
2FI	0.14	6	0.024	1.95	0.2692	
Quadratic	0.038	3	0.013	1.05	0.4616	
Cubic	0.000	0				Aliased
Pure Error	0.048	4	0.012			

"Lack of Fit Tests": Want the selected model to have insignificant lack-of-fit.

Model Summary Statistics

Source	Std. Dev.	R-Squared	Adjusted R-Squared	Predicted R-Squared	PRESS	
Linear	0.15	0.8642	0.8329	0.7498	0.53	**Suggested**
2FI	0.14	0.9099	0.8558	0.6782	0.68	
Quadratic	0.11	0.9590	0.9062	0.6746	0.69	
Cubic	0.11	**0**.9771	0.9082		+	**Aliased**

+ Case(s) with leverage of 1.0000: PRESS statistic not defined

Appendix 3: ANOVA for the response (Dielectric strength)

Process order: Modified

Selection: Stepwise

Response:Dielectric strength Transform:Square rootConstant: 0

Stepwise Regression with Alpha to Enter = 0.100, Alpha to Exit = 0.100

Forced Terms Intercept

Added	Coefficient Estimate	t for H0 Coeff=0	Prob > |t|	R-Squared	MSE
A	0.47	8.45	<0.0001	0.8265	0.024
BC	0.15	2.20	0.0452	0.8710	0.019
A2	0.14	2.33	0.0367	0.9089	0.015
B	0.084	2.23	0.0458	0.9356	0.011

ANOVA for Response Surface Reduced Quadratic Model

Analysis of variance table [Partial sum of squares]

Source	Sum of Squares	DF	Mean Square	F Value	Prob > F	
Model	1.99	5	0.40	39.08	< 0.0001	significant
A	*1.74*	*1*	*1.74*	*170.56*	*< 0.0001*	
B	*0.056*	*1*	*0.056*	*5.50*	*0.0388*	
C	*0.023*	*1*	*0.023*	*2.30*	*0.1579*	
A^2	*0.080*	*1*	*0.080*	*7.83*	*0.0173*	
BC	*0.094*	*1*	*0.094*	*9.19*	*0.0114*	
Residual	0.11	11	0.010			
Lack of Fit	*0.064*	*7*	*9.138E-003*	*0.76*	*0.6503*	*not significant*
Pure Error	*0.048*	*4*	*0.012*			
Cor Total	2.11	16				

The Model F-value of 39.08 implies the model is significant. There is only a 0.01% chance that a "Model F-Value" this large could occur due to noise.

Values of "Prob > F" less than 0.0500 indicate model terms are significant. In this case A, B, A2, BC are significant model terms.

Values greater than 0.1000 indicate the model terms are not significant. If there are many insignificant model terms (not counting those required to support hierarchy), model reduction may improve your model.

The "Lack of Fit F-value" of 0.76 implies the Lack of Fit is not significant relative to the pure error. There is a 65.03% chance that a "Lack of Fit F-value" this large could occur due to noise. Non-significant lack of fit is good -- we want the model to fit.

Std. Dev.	0.10	R-Squared	0.9467
Mean	7.89	Adj R-Squared	0.9225
C.V.	1.28	Pred R-Squared	0.8889
PRESS	0.23	Adeq Precision	18.335

The "Pred R-Squared" of 0.8889 is in reasonable agreement with the "Adj R-Squared" of 0.9225.

"Adeq Precision" measures the signal to noise ratio. A ratio greater than 4 is desirable. Your ratio of 18.335 indicates an adequate signal. This model can be used to navigate the design space.

Factor	Coefficient Estimate	DF	Standard Error	95% CI Low	95% CI High	VIF
Intercept	7.83	1	0.034	7.75	7.90	
A-Sintering Temperature	0.47	1	0.036	0.39	0.55	1.00
B-Pressing pressure	0.084	1	0.036	5.133E-003	0.16	1.00
C-Soaking Time	0.054	1	0.036	-0.024	0.13	1.00
A2	0.14	1	0.049	0.029	0.25	1.00
BC	0.15	1	0.051	0.042	0.26	1.00

Final Equation in Terms of Coded Factors:

Sqrt(Dielectric strength) =

+7.83
+0.47 * A
+0.084 * B
+0.054 * C
+0.14 * A2
+0.15 * B * C

Final Equation in Terms of Actual Factors:

Sqrt(Dielectric strength) =

+103.47833
-0.14454 * Sintering Temperature
-0.022253 * Pressing pressure
-0.71159 * Soaking Time
+5.49536E-005 * Sintering Temperature 2
+0.015314 * Pressing pressure * Soaking Time

Appendix 4: 3D and contour plots for the response

A)

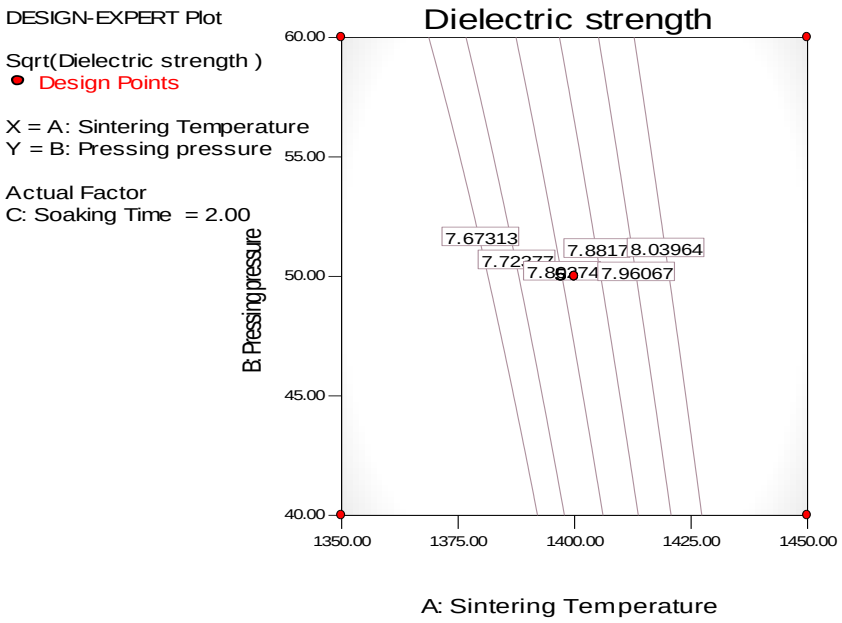

B)

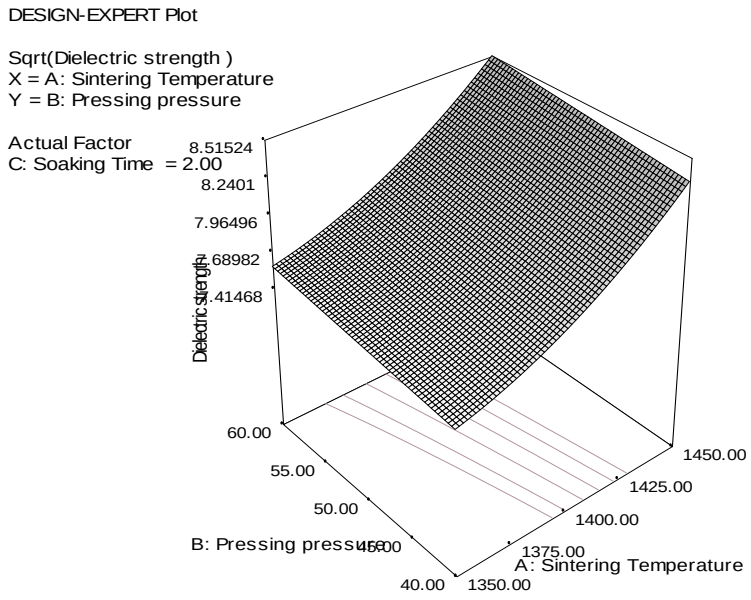

Figure A4 1 Three-dimensional 3D response surface and contour plot showing the effect of sintering Temperature and Pressing Pressure and Soaking Time fixed at 2.00 Hr. A)Contour and B) 3Dsurface response respectively.

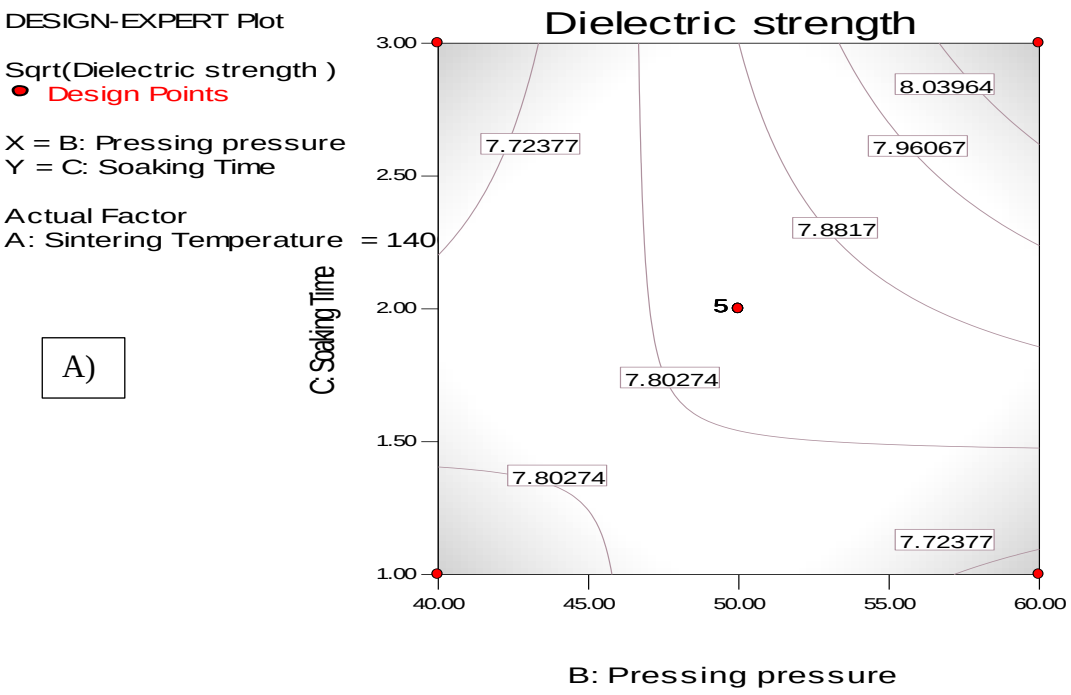

A)

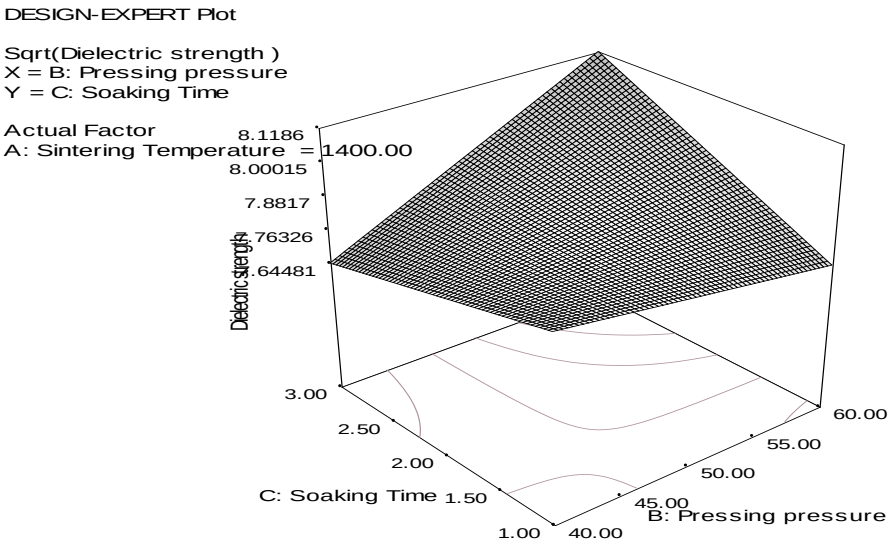

B)

Figure A4 2 Three-dimensional 3D response surface and contour plot showing the effect of Soaking Time and Pressing Pressure and Sintering Temperature fixed at 1400°c A) contour and B) 3Dsurface response.

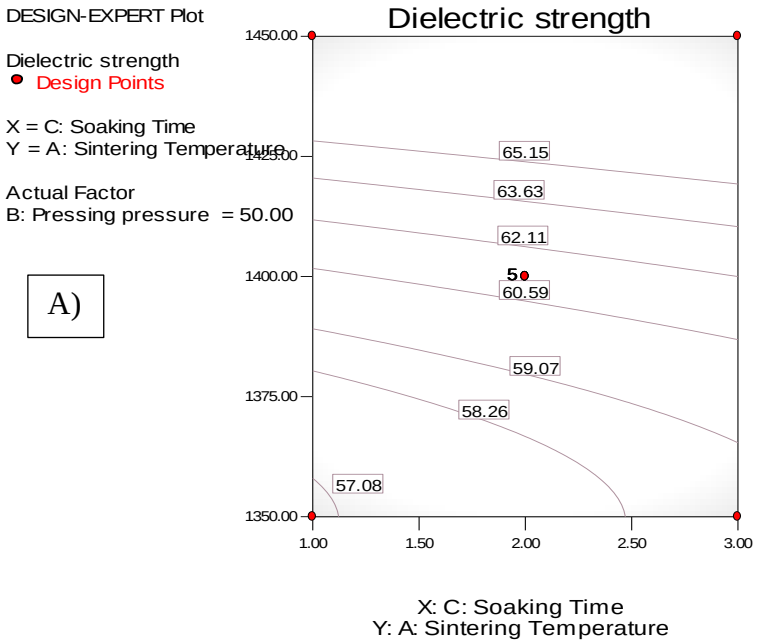

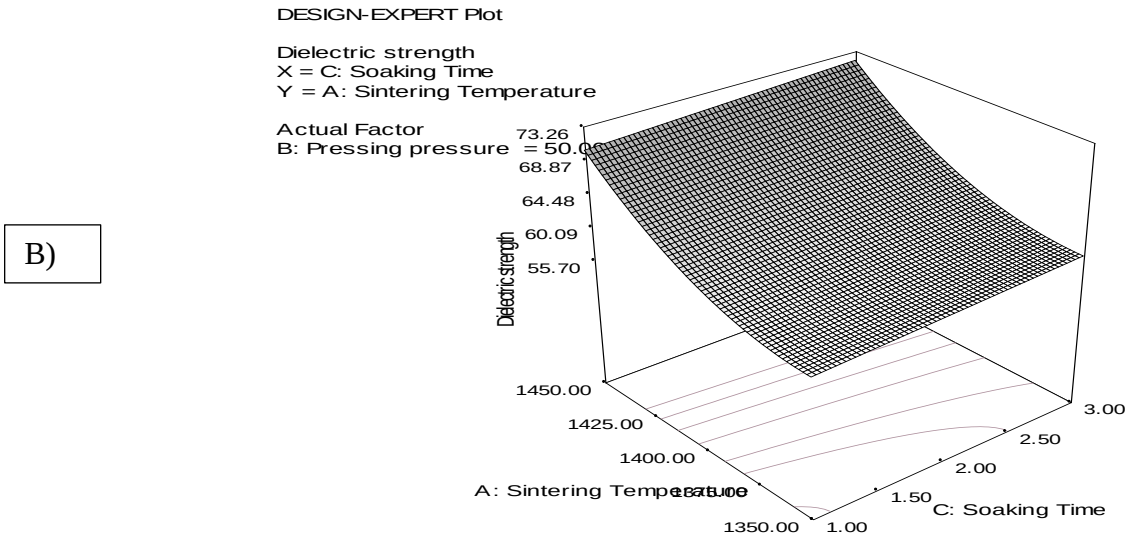

Figure A4 3 Three-dimensional 3D response surface and contour plot showing the effect of Soaking Time and Sintering Temperature and Pressing Pressure fixed at 50KPa A) contour and B) 3Dsurface response.

Appendix-5: pictures during the research work

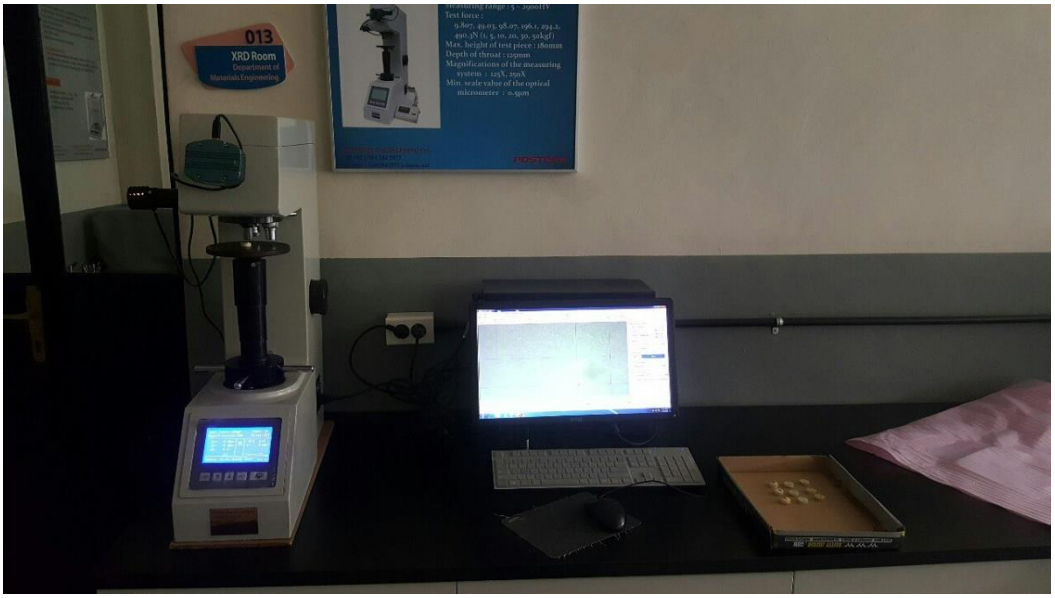

FigureA5. 1 Vickers Hardness Tester for measuring the hardness of the sample

FigureA5. 2 Suspended mass measurement in the laboratory

FigureA5. 3 The sample boiled in the distilled water

FigureA5. 4 The sample in the furnace

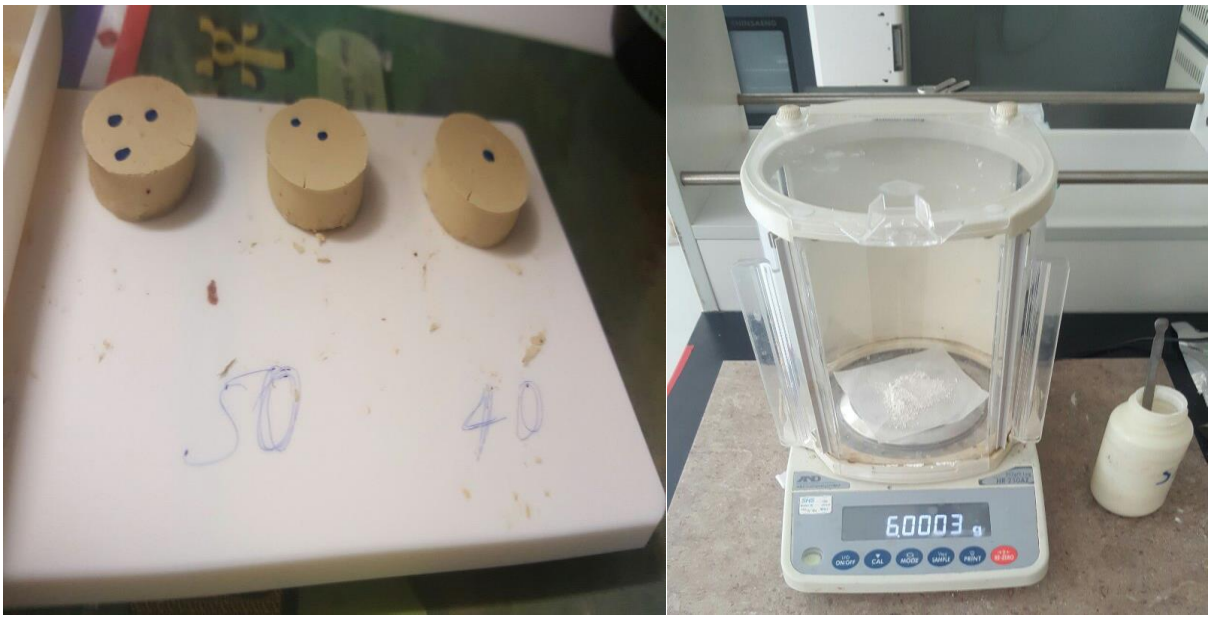

FigureA5. 5 The sample after sintering and the powder weigh up in electrical balance

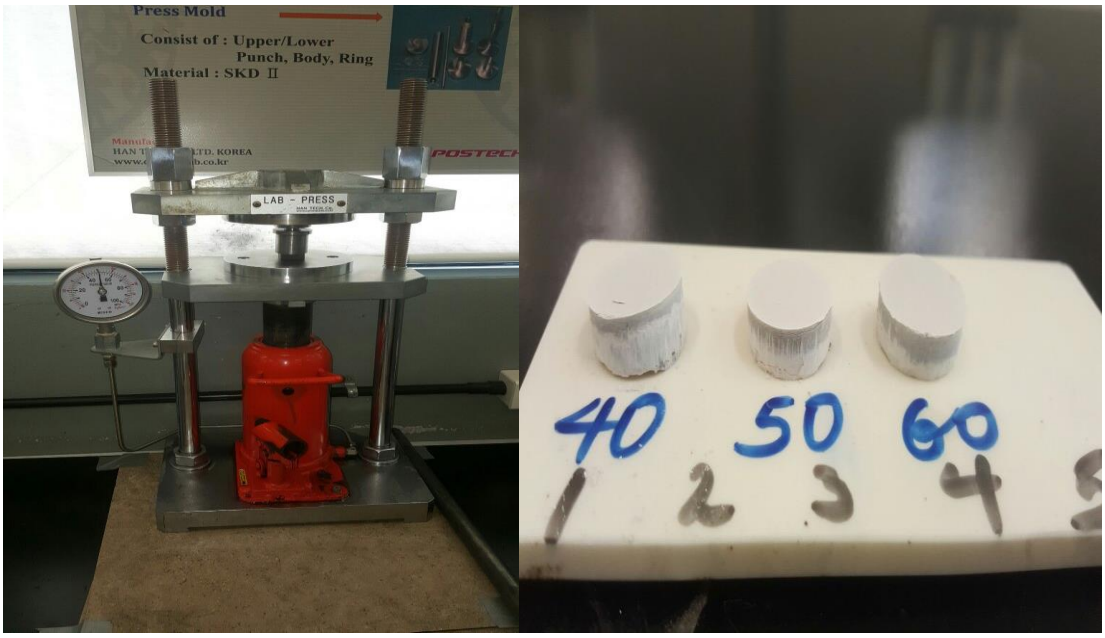

FigureA5. 6 The sample molded in the press mold and pressed specimens.

FigureA5. 7 Ball mill machine for milling and mixing

FigureA5. 8 The specimen in forced convection drying oven